Revisiting Percolation Models of Capillary Hysteresis

Alexander V. Neimark
Credits: Richard Cimino, Rutgers University
Katie Cychosz and Matthias Thommes, Quantachrome Instruments

aneimark@rutgers.edu, http://sol.rutgers.edu/~aneimark

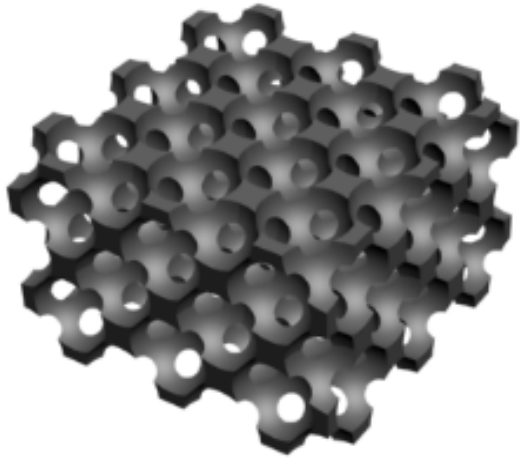

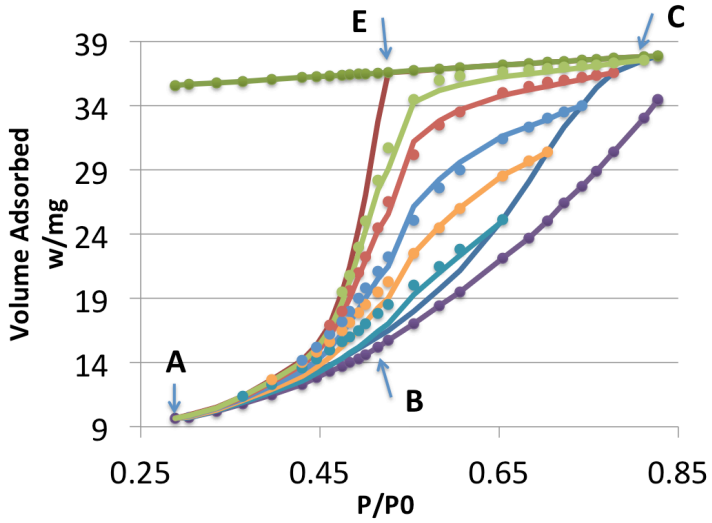

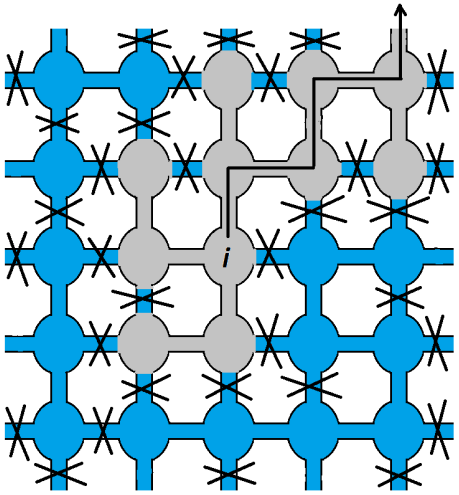

Honoring Giorgio Zgrablich

Theoretical and experimental studies of capillary condensation hysteresis in pore networks

One of the most long-studied and still enigmatic problem in adsorption science

Classical period:

1911-1967 - Zsigmondy, Kraemer, Cohan, McBain, deBour, Dubinin, Everett, … - Elementary mechanisms based on classical thermodynamics for cylindrical and ink-bottle pores – delayed condensation, pore blocking, tensile stress limit, cavitation

J. H. de Boer, in The Structure and Properties of Porous Materials, ed. D. H. Everett and F. S. Stone, Butterworths, London, 1958, vol. 10, p. 95.

D. H. Everett, in The Solid- Gas Interface, ed. E. A. Flood, Marcel Dekker, New York, 1967, vol. 2, ch.36, pp. 1055–1113.

Independent Domain Theory

Modern period:

1981 – Percolation Theory of Hysteresis in Pore Networks - Wall&Braun, Mason, Maygotia, Zgrablich, Rojas, Ricardo …

1986 – DFT, Molecular Simulations – Evans, Gubbins, Monson, Do, …

Theoretical and experimental studies of capillary condensation hysteresis in pore networks

Motivation for revisiting percolation models:

- New experiments on well-characterized materials, including scanning isotherms
- Scanning hysteresis loop brings about additional information about the pore structure
- Measurements became high precision and routine
- Luck of quantitative theory that can be used for pore structure analysis

OUTLINE

Experimental examples – what we want to understand
Physical mechanisms of hysteresis
Models of independent pores – how to distinguish networking effects
Pore blocking/percolation effects – network theory of scanning isotherms
Calculating network connectivity and pore size distribution

EARLIER WORK: Neimark A.V. - Rep. Acad. Sci. USSR., 1983, v. 273, 384
Colloid J. of the USSR, 1984, v. 46, 927;1158.

Capillary Hysteresis in Porous Materials - Examples

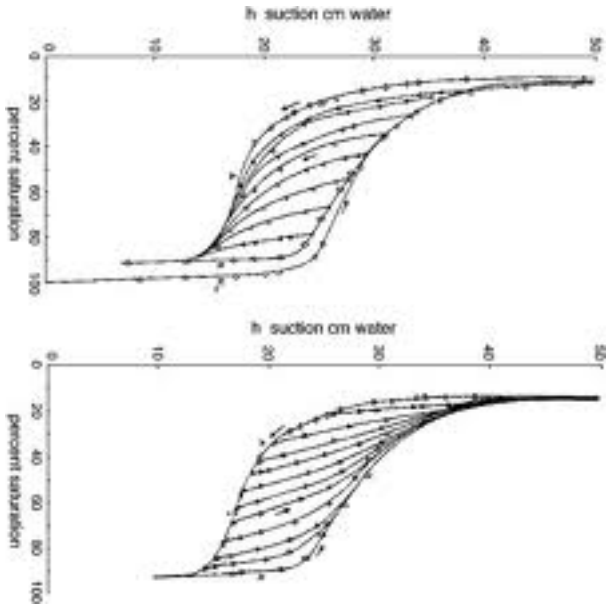

Imbibition and drainage
Pop et al, 2009

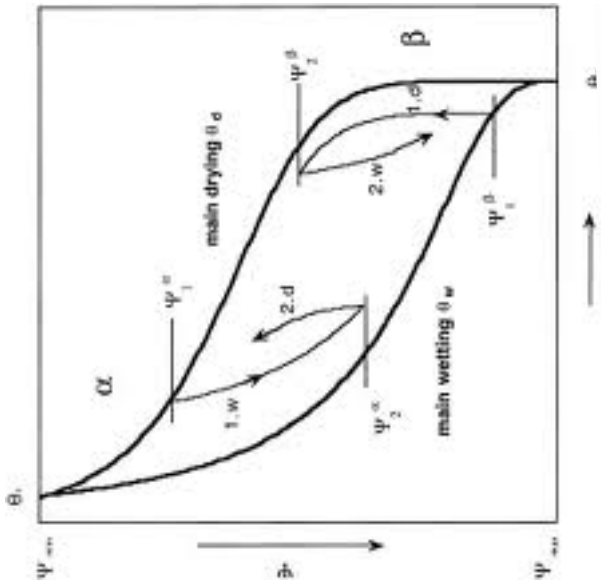

Wetting and drying
Lehmann et al, 1998

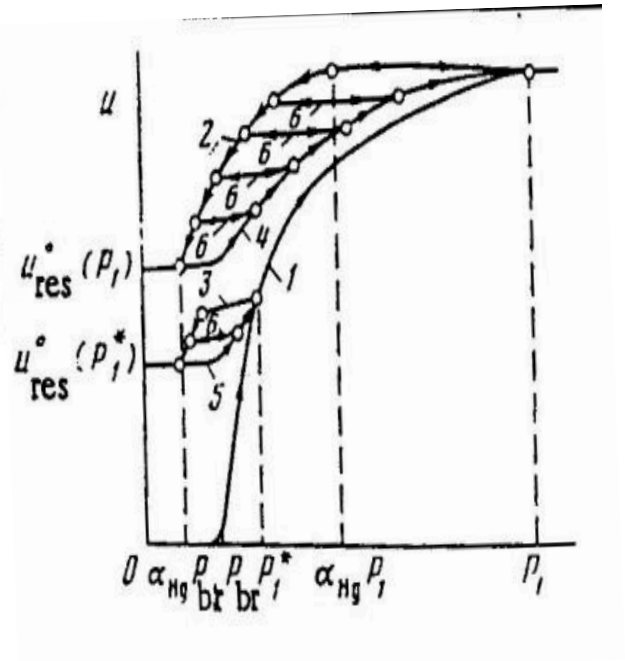

Intrusion and extrusion
Neimark, 1985

Specifics of capillary hysteresis are determined by interplay of wetting/adsorption properties and pore geometry

Objective: theoretical and experimental studies of capillary condensation hysteresis in pore networks of well-characterized materials

Richard Cimino, Katie Cychosz, Matthias Thommes, and AVN, CPM-6, 2012

Typical capillary condensation hysteresis in porous materials

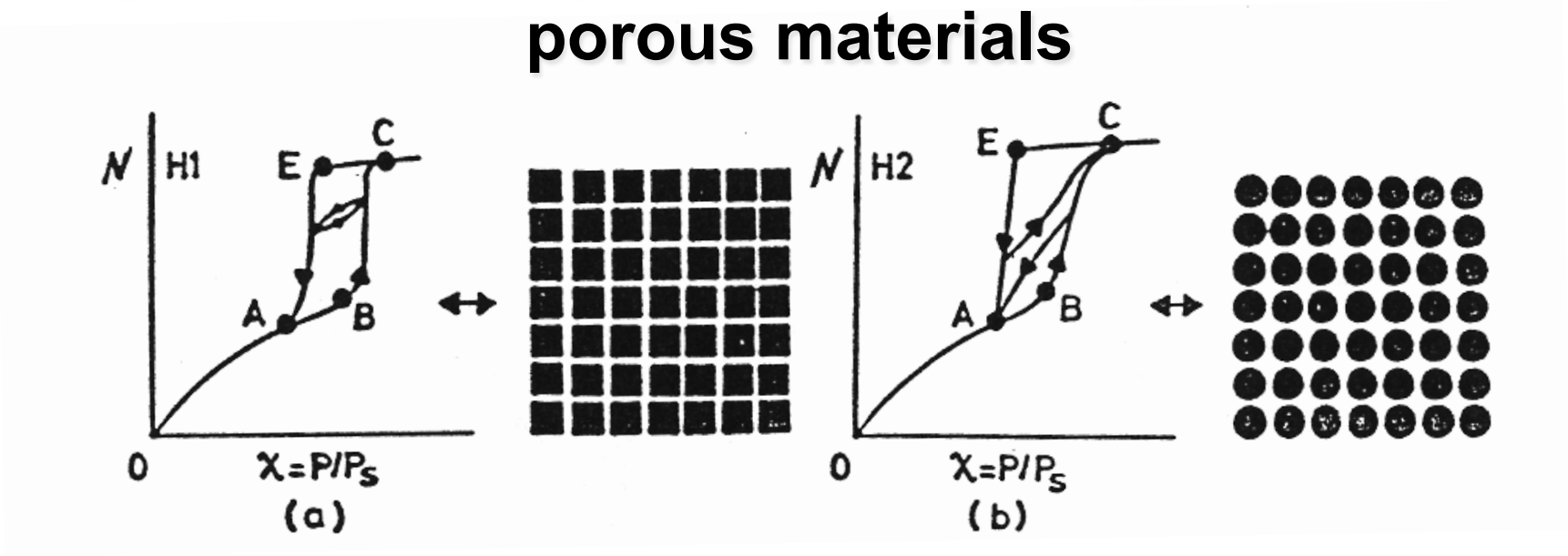

Two characteristic types of hysteresis behavior:

H1 – Scanning isotherms form close loops crossing the main hysteresis loop characteristic for networks of channels

H2 – Scanning isotherms approaching the upper and lower point of closure of the main hysteresis loop characteristic for networks of cage-like pores with narrow necks

Characteristic points:

A – lower limit of hysteresis;

B – beginning of irreversible capillary condensation;

C – upper limit of hysteresis;

E – beginning of irreversible evaporation

AVN, COPS-2, 1990

Theoretical and experimental studies of capillary condensation hysteresis with reference well-characterized materials

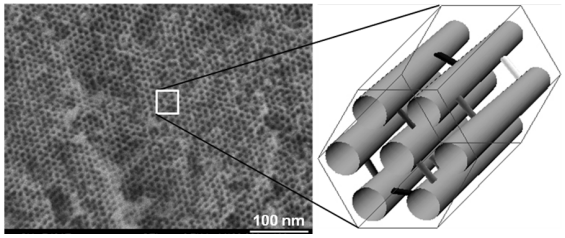

SBA-15 silica – regular hexagonal array of cylindrical channels

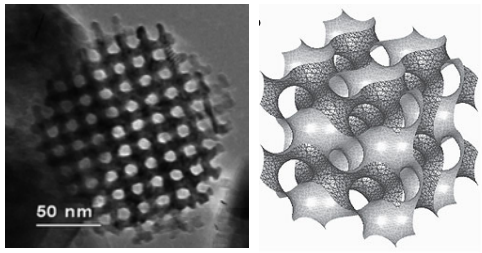

KIT-6 silica – regular 3D cubic gyroid pore network

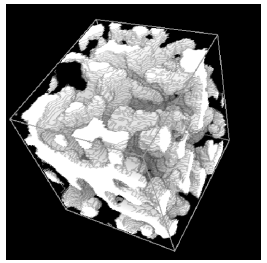

Vycor glass – disordered 3D pore network

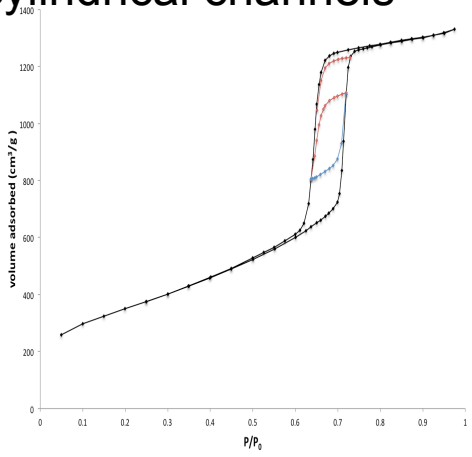

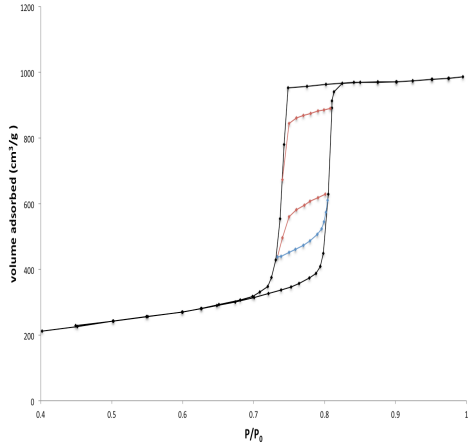

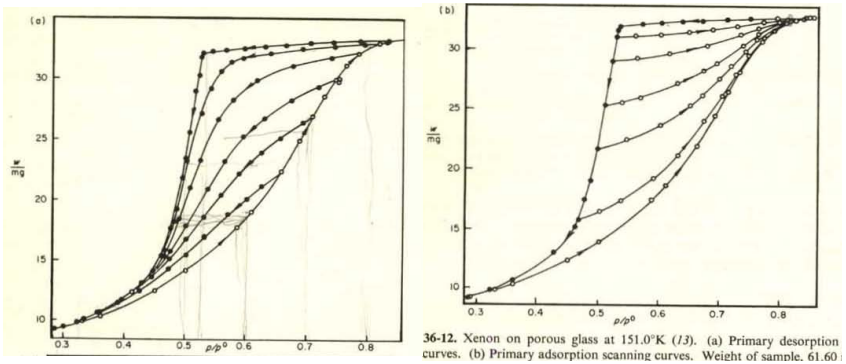

36-12. Xenon on porous glass at 151.0°K (*13*). (a) Primary desorption curves. (b) Primary adsorption scanning curves. Weight of sample, 61.60

Two characteristic types of scanning hysteresis behavior:

-Close loops within main H1 type hysteresis loop characteristic for SBA-15 and KIT-6

-Scanning isotherms approaching the upper and lower point of closure of main H2 type hysteresis loop characteristic for Vycor (from Everett, 1967).

Novel 3D Ordered Mesoporous Carbons – 3DOm

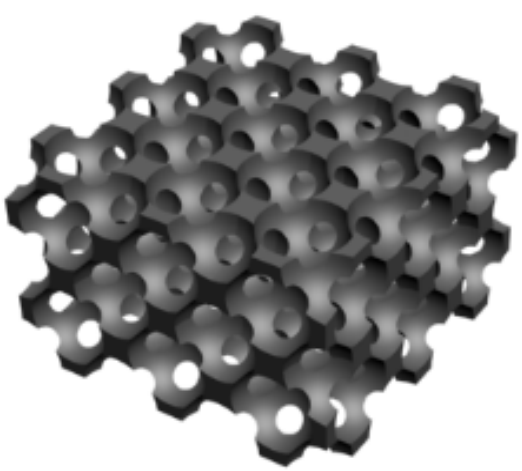

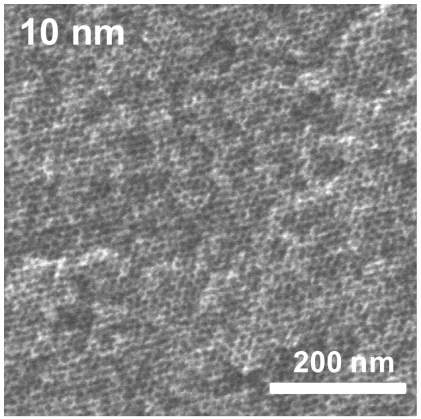

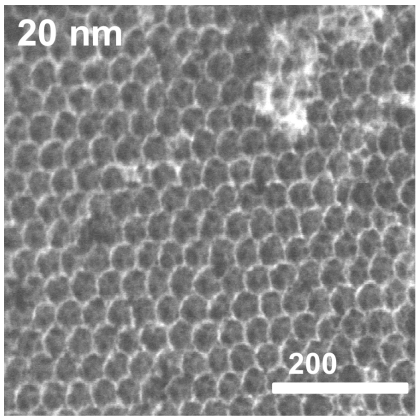

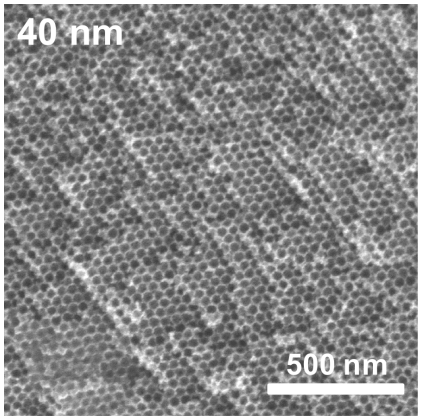

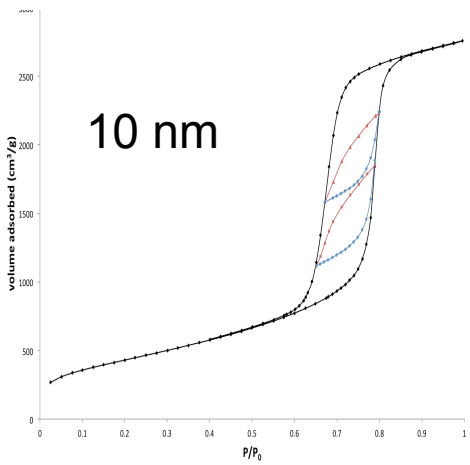

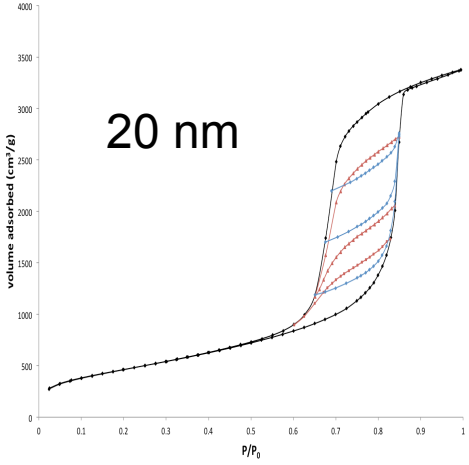

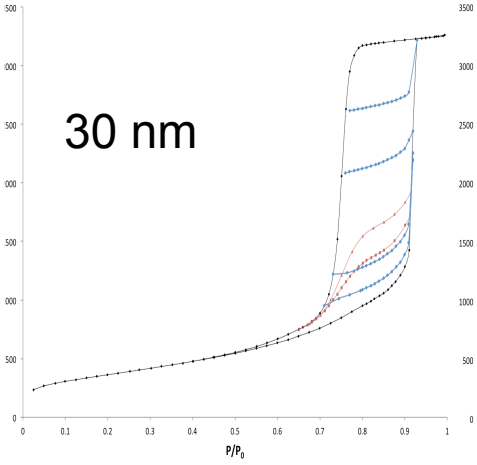

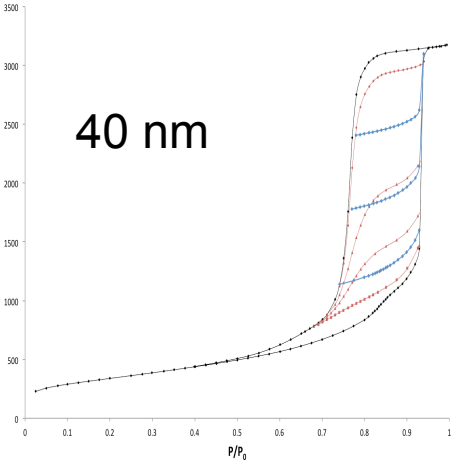

Obtained by templating of 3D colloidal crystals of silica nanoparticles - Tsapasis.
Cubic network of cage-like pores connected by narrow necks/windows.
4 samples templated on particles of 10 nm, 20 nm, 30 nm and 40 nm.

Capillary hysteresis: classical description of delayed condensation

Wetting liquid film inside cylindrical capillary

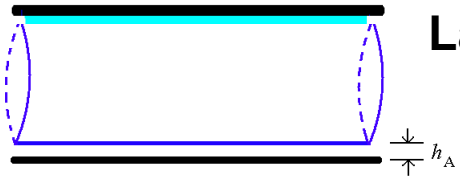

Laplace equation for cylindrical interface

$$\Delta P = -\frac{\gamma}{R}$$

Meniscus inside cylindrical capillary

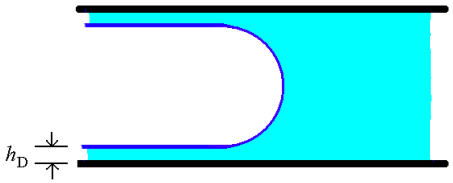

Laplace equation for spherical interface

$$\Delta P = -\frac{2\gamma}{R}$$

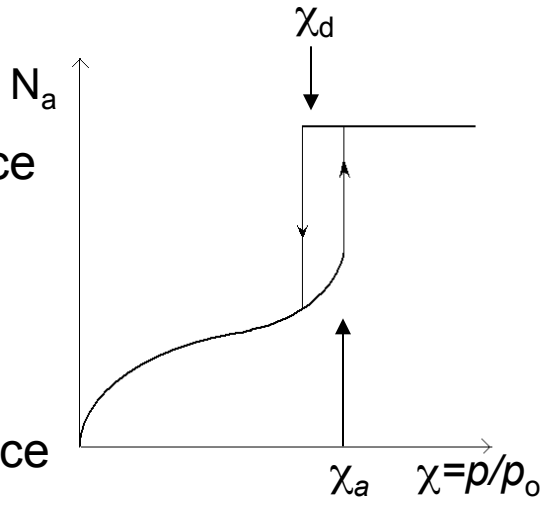

Capillary condensation is described by **Kelvin** equation for cylindrical interface between adsorbed film and vapor

$$R_T T \ln \chi_a = -\frac{\gamma v_L}{R}$$

Evaporation/desorption is described by **Kelvin** equation for hemispherical meniscus between condensed fluid and vapor

$$R_T T \ln \chi_d = -\frac{2\gamma v_L}{R}$$

Deterministic model: pressures of capillary condensation and evaporation are strictly correlated; both are determined by the pore size

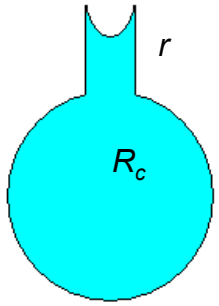

Adsorption in ink-bottle pores

Pore blocking effect on the single pore level

1931-1967
Kraemer, McBain, Cohan, de Bour, Everett, Dubinin

Condensation

Delayed condensation: fluid condenses in a pore of size R_P at the relative pressure determined from the equilibrium condition for the adsorption film on spherical surface of R_P

$$RT \ln \chi_a = -\frac{2\gamma V_L}{R_P}$$

Desorption

Classical pore blocking effect: fluid condensed in a pore can evaporate only the evaporation occurs in at least one of its necks: the desorption pressure is determined by the size of the neck *r*.

$$RT \ln \chi_d = -\frac{2\gamma V_L}{r}$$

Cavitation: If the necks are very narrow (<~4nm), condensed fluid achieves the limit of thermodynamic stability, tensile stress limit, and spontaneously boils: the desorption pressure does not depend on the pore size.

Two parameter model: pressures of capillary condensation and evaporation are not necessarily correlated.

Uncorrelated model is common.

Cooperative effects during adsorption and desorption

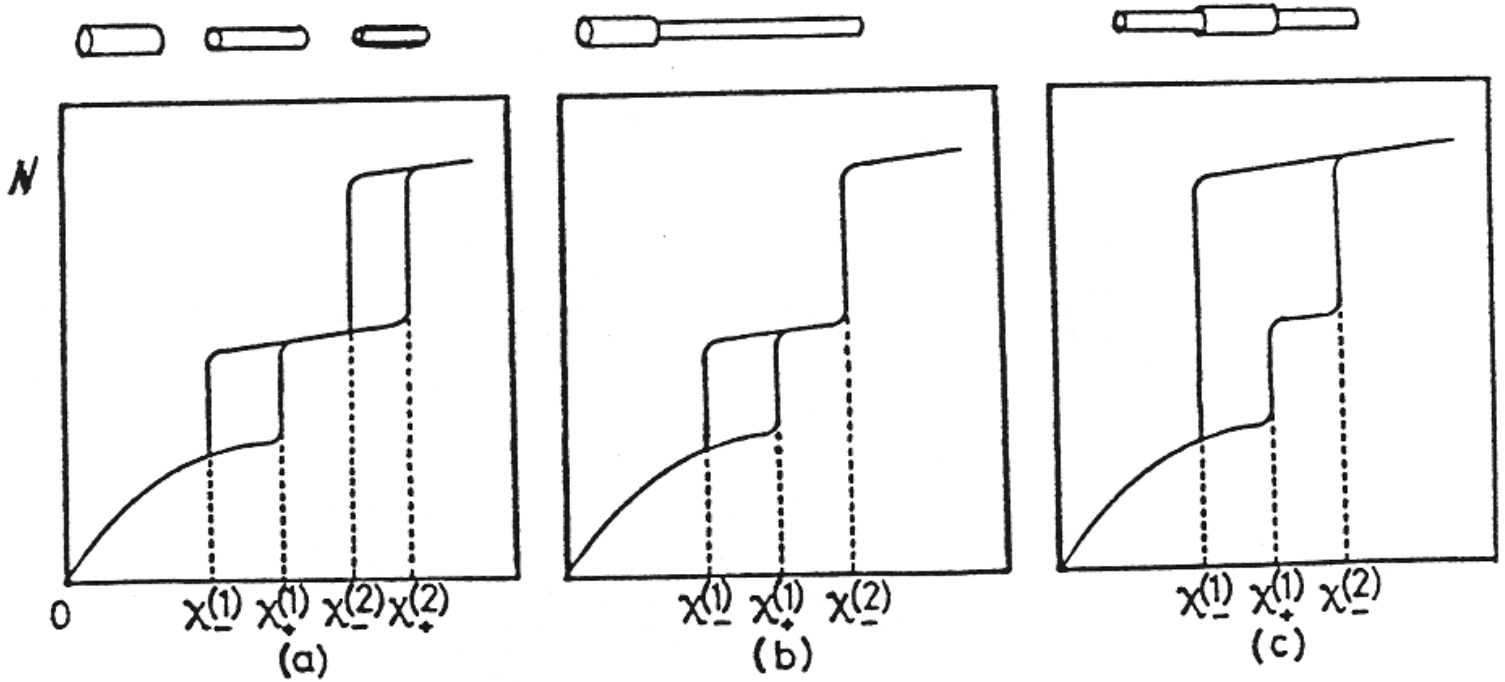

Hysteresis loops in a model system of three capillaries.

AVN, COPS-2, 1990

Network effects:

1. **Initiation of capillary condensation**
2. **Delay of desorption due to pore-blocking**
3. **Cavitation** (introduced in percolation model by Parlar&Yortsos, 1988)
4. **Complex pore networks where these mechanisms interplay** (dual pore model , 1985 – Mayagoitia, Zgrablich, Rojas, Ricardo, …)

Dual-Pore Model

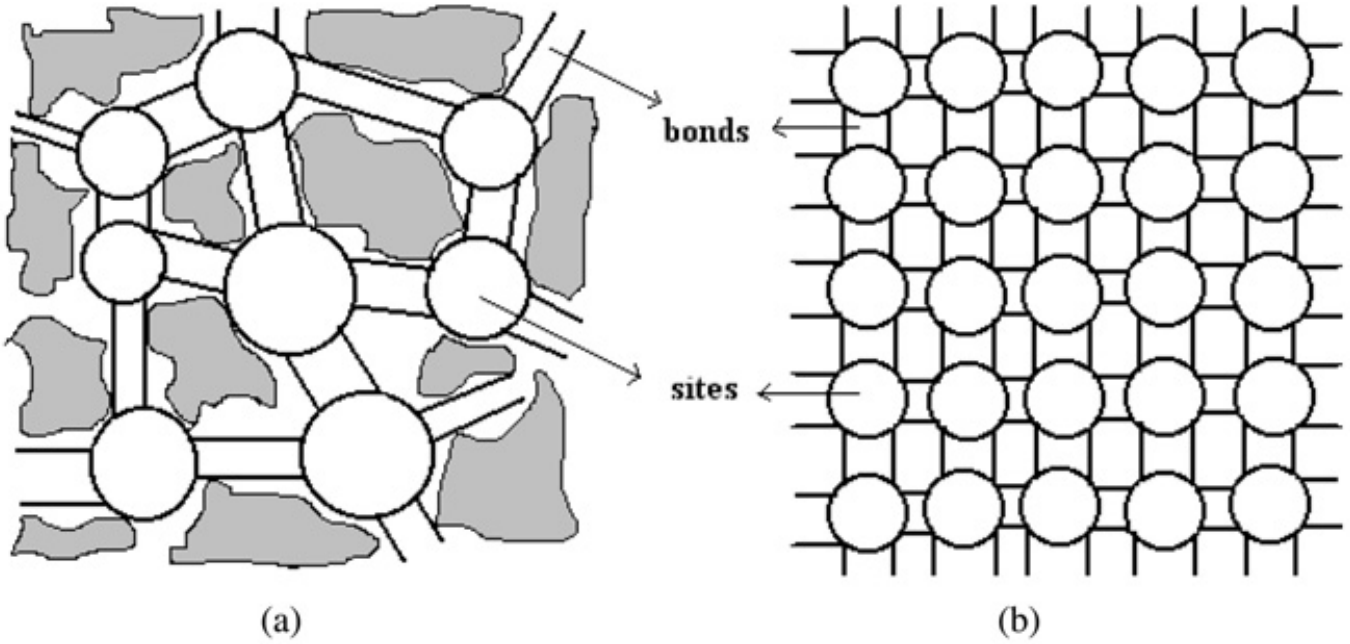

Introduced in 1985 – Mayagoitia, Rojas and Kornhauser
Advanced and applied In Mexico and San Luis group by Zgrablich, Ricardo, and their colleagues.
Scanning hysteresis – Rojas et al, Phys. Chem. Chem. Phys., 2002, 4, 2346–2355

Main question to be addressed in any theoretical model:
What is the probability that a pore of given size d_p is filled at given vapor pressure χ ?
This probability determines the isotherm in terms of fractions of filled and unfilled pores.
Hysteresis implies that this probability depends on the history of the adsorption-desorption process; it is different for adsorption, desorption, and scanning isotherms.

How to treat isotherms: from saturation to fractions of unfilled and filled pores

$$V(\chi) = Q(\chi) \cdot V_s(\chi) + (1 - Q(\chi)) \cdot V_c(\chi)$$

$V(\chi)$ – saturation at partial pressure $\chi = p/p_0$

$Q(\chi)$ – **fraction of unfilled pores**

$V_s(\chi)$ – reference isotherm in unfilled pores

$V_s(\chi) = S \cdot h(\chi)$ = surface area · film thickness

$V_c(\chi)$ – reference isotherm in filled pores approximated by linear compressibility

$$Q(\chi) = \frac{V_c(\chi) - V(\chi)}{V_c(\chi) - V_s(\chi)}$$ - general relation

$$Q_+(\chi) = \frac{V_c(\chi) - V_+(\chi)}{V_c(\chi) - V_s(\chi)}$$ - main adsorption

$$Q_-(\chi) = \frac{V_c(\chi) - V_-(\chi)}{V_c(\chi) - V_s(\chi)}$$ - main desorption

New: introduction of reference isotherms

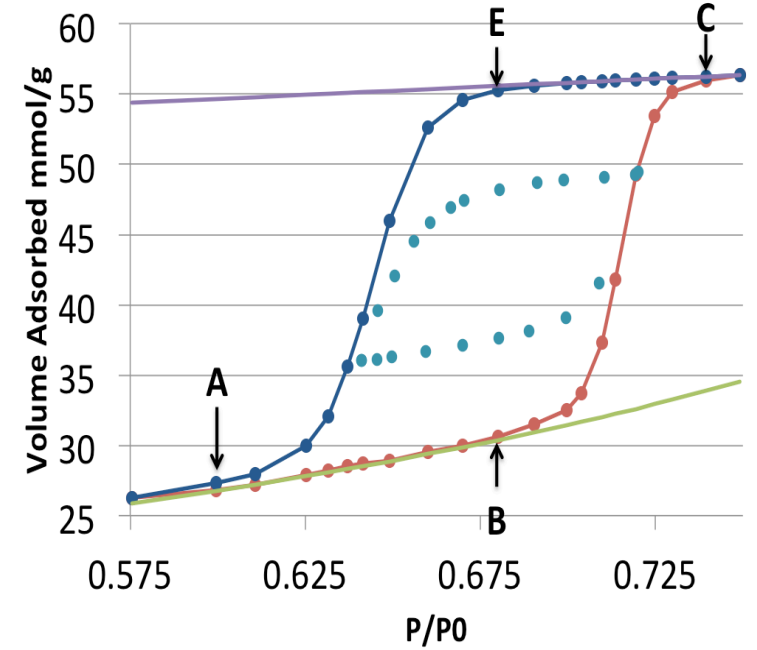

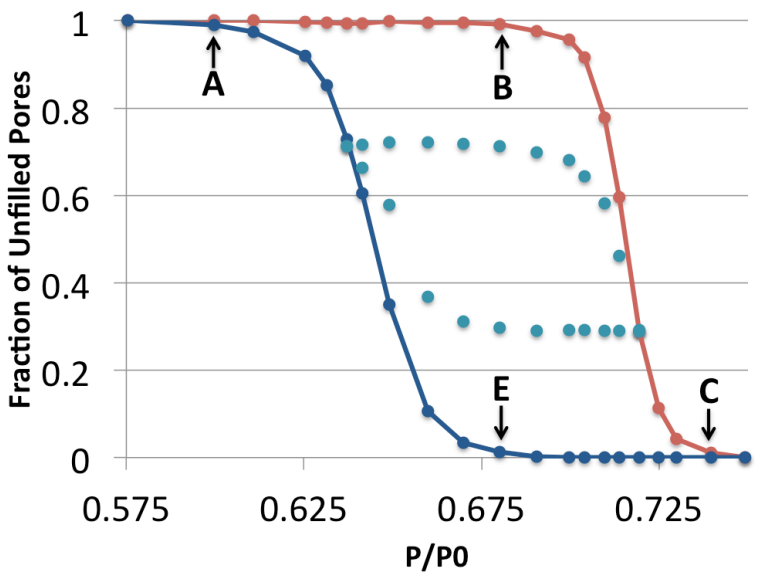

Independent pores: Deterministic and Uncorrelated Model

Deterministic model: pressures of capillary condensation, and evaporation are strictly correlated; both are determined by the pore size: $\chi_a = \chi_a(d_p)$; $\chi_d = \chi_d(d_p)$
Sequence of pore filling along adsorption isotherm is from small pores to large
Sequence of pore emptying along desorption isotherm is reverse from large to small

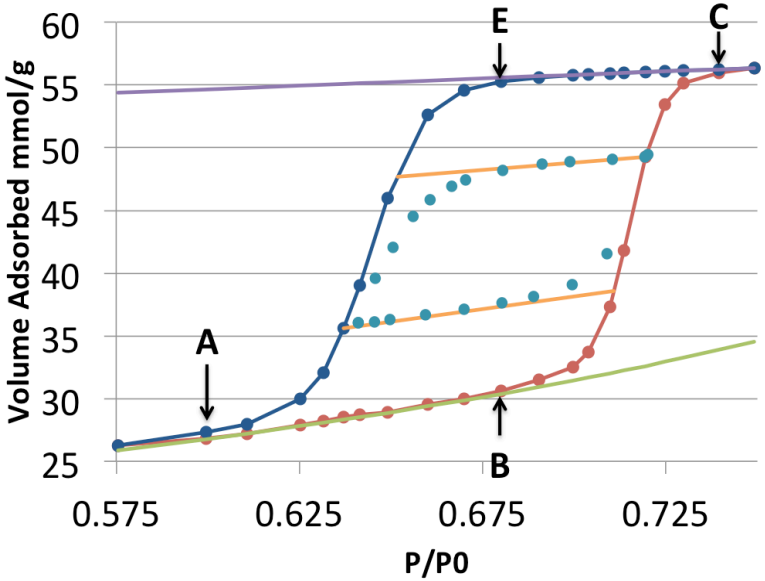

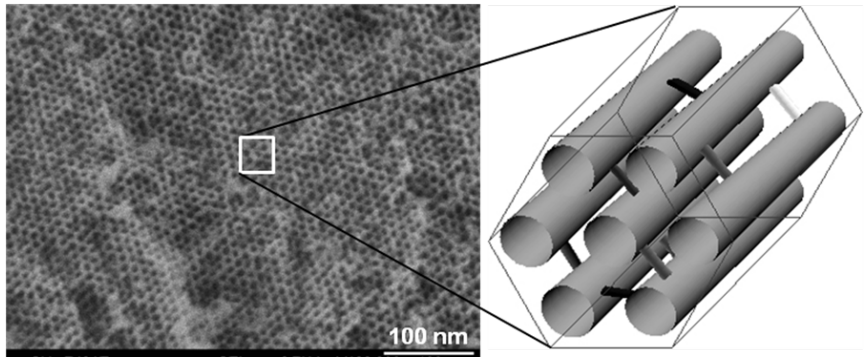

$$Q_-(\chi, \chi_a) = Q_+(\chi_a)$$

Fraction of unfilled pores during scanning adsorption started at $\chi = \chi_a$

$$Q_+(\chi, \chi_d) = Q_-(\chi_d)$$

Fraction of unfilled pores during scanning desorption started at $\chi = \chi_d$

Conclusion from the deterministic model of independent pores:
Scanning isotherm must connect the points on adsorption and desorption isotherms, which correspond to the same fraction of unfilled pores (orange lines).

Does not work even for most ideal pore structure of SBA-15!

Independent pores: Deterministic and Uncorrelated Model

Uncorrelated model: pressures of capillary condensation and evaporation are not correlated. Pore filling is determined by the pore size d_p, pore emptying is determined by the neck size d_n, which are not correlated: $\chi_a = \chi_a(d_p)$ $\chi_d = \chi_d(d_n)$

Sequence of pore filling along adsorption isotherm is from small pores to large

Sequence of pore emptying along desorption isotherm is determined by the largest neck

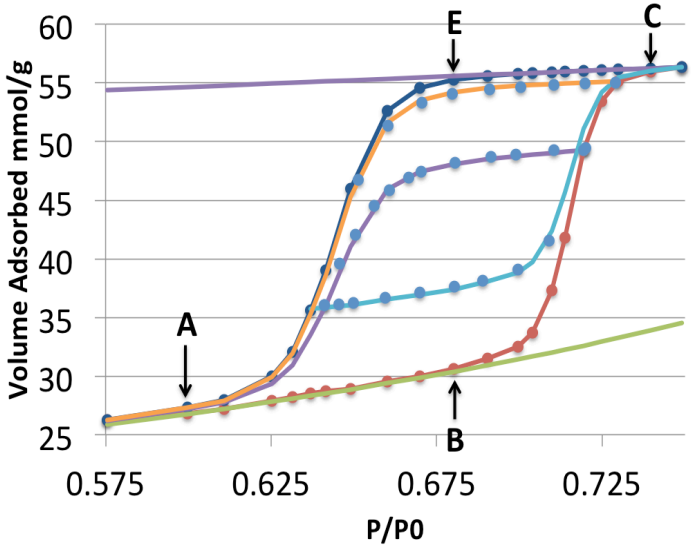

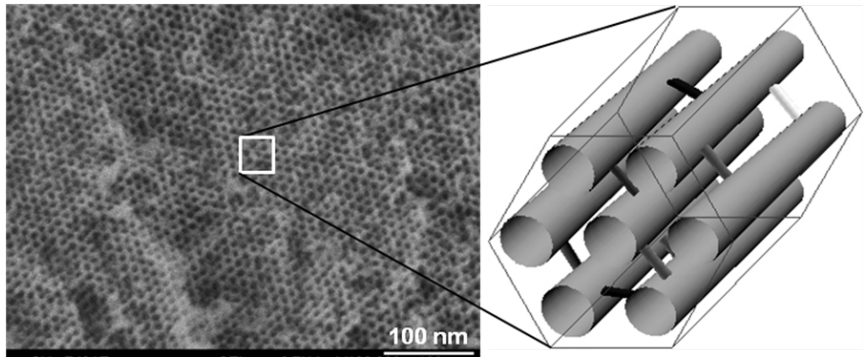

$$Q_+(\chi, \chi_d) = Q_+(\chi) \cdot Q_-(\chi_d) \qquad Q_-(\chi, \chi_a) = 1 - \left(1 - Q_-(\chi)\right) \cdot \left(1 - Q_+(\chi_a)\right)$$

Fraction of unfilled pores during scanning adsorption started at $\chi = \chi_a$

Fraction of unfilled pores during scanning desorption started at $\chi = \chi_d$

Conclusion from the uncorrelated model:

Scanning isotherms must terminate at the points of closure of the main hysteresis loop

Works better that deterministic model for SBA-15!

Independent pore model provides a test for percolation effects

Uncorrelated model: pressures of capillary condensation and evaporation are not correlated.

Sequence of pore filling along adsorption isotherm is from small pores to large

Sequence of pore emptying along desorption isotherm is determined by the largest neck

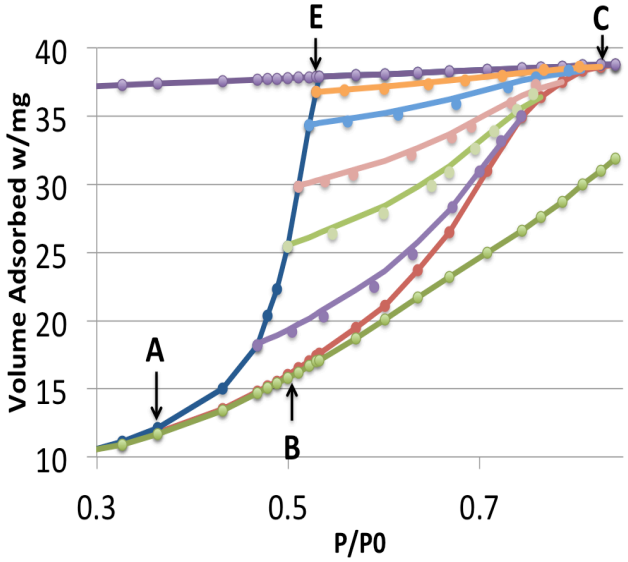

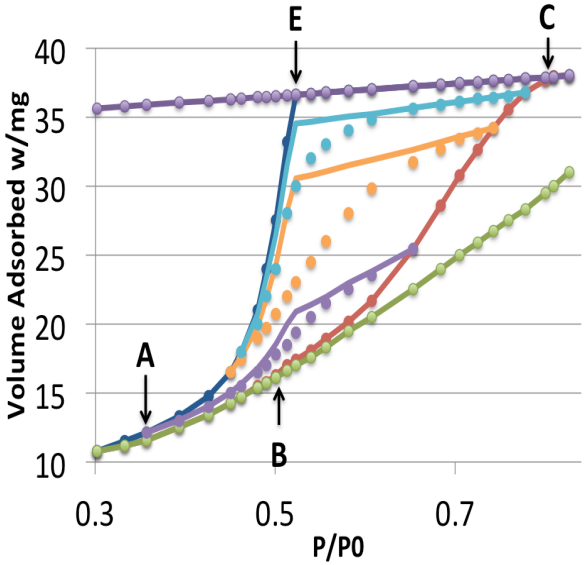

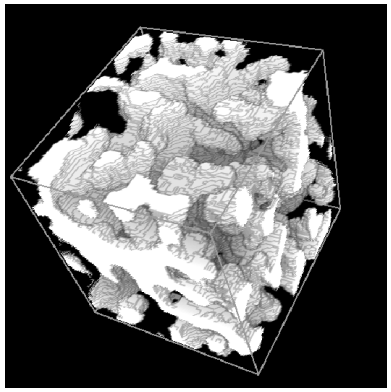

$$Q_+(\chi,\chi_d) = Q_+(\chi)\cdot Q_-(\chi_d)$$

Fraction of unfilled pores during scanning adsorption started at $\chi = \chi_a$

$$Q_-(\chi,\chi_a) = 1-\left(1-Q_-(\chi)\right)\cdot\left(1-Q_+(\chi_a)\right)$$

Fraction of unfilled pores during scanning desorption started at $\chi = \chi_d$

Scanning isotherms must terminate at the points of closure of the main hysteresis loop

Works for scanning adsorption,

but not for scanning desorption due to percolation effects!

In agreement with earlier work, Neimark, 1983

Independent pores: Partial Correlation Model (PCM)

Pressures of capillary condensation and evaporation are partially correlated.
Pore filling is determined by the pore size, pore emptying is determined by the neck size.
The larger the pore the larger the neck!

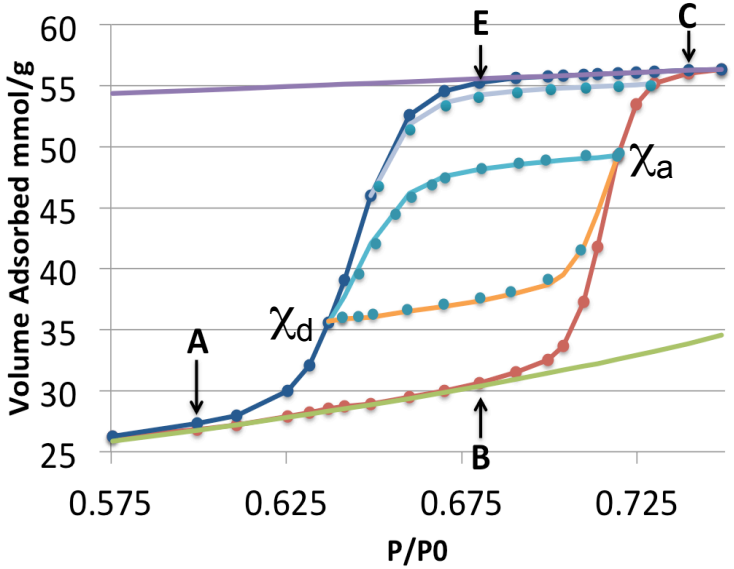

A – lower closure
B – onset of capillary condensation
C – upper closure
E – onset of capillary evaporation

If scanning adsorption and desorption isotherms form a close loop crossing the main loop at $\chi = \chi_d$ and at $\chi = \chi_a$, all pores larger than $d_p(\chi_d)$ must have necks larger than $d_n(\chi_a)$

Independent pores: Partial Correlation Model

For scanning adsorption starting at $\chi = \chi_d$ and approaching adsorption boundary at $\chi = \chi_a$:

$$Q_+(\chi, \chi_d) = Q_-(\chi_d) - \left(Q_-(\chi_d) - Q_+(\chi_a)\right)\left(\left(1 - Q_+(\chi)\right)\Big/\left(1 - Q_+(\chi_a)\right)\right)$$

For scanning desorption starting at $\chi = \chi_a$ and approaching desorption boundary at $\chi = \chi_d$:

$$Q_-(\chi, \chi_a) = Q_+(\chi_a) + \left(Q_-(\chi_d) - Q_+(\chi_a)\right)\left(Q_-(\chi)/Q_-(\chi_d)\right)$$

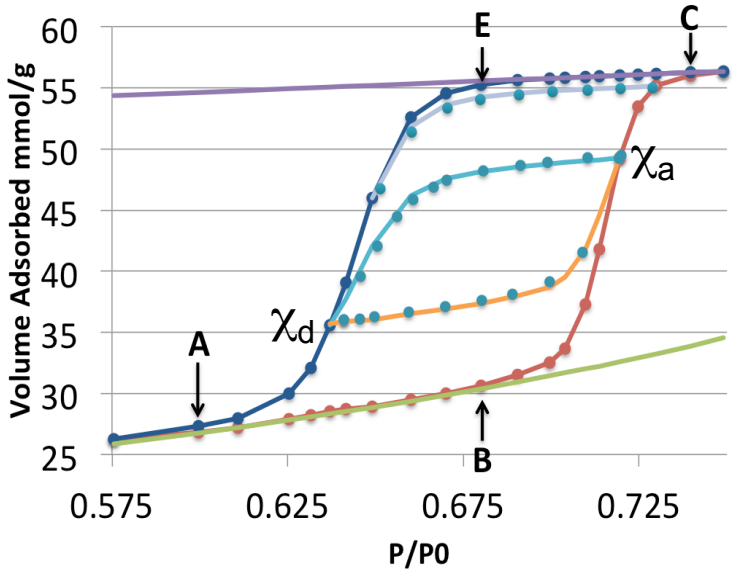

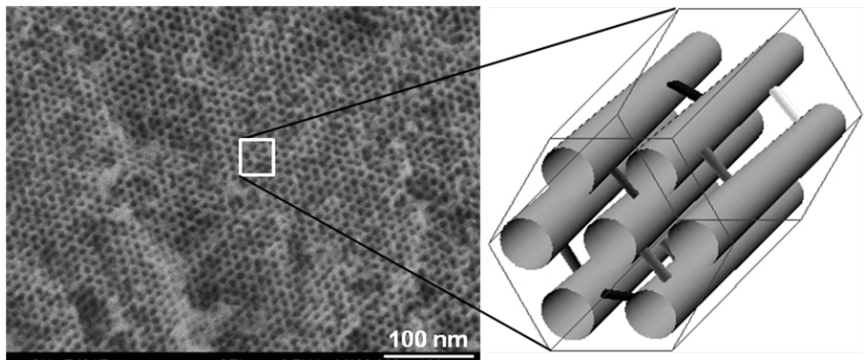

Works perfectly for SBA-15!

Adsorption and desorption isotherms form close loops crossing the main hysteresis loop.
Possible explanation – pore channels are corrugated

in agreement with earlier work of Giorgio Zgrablich, Esparza et al, 2004 .

Partial correlation model provides a test for percolation effects

KIT-6 silica

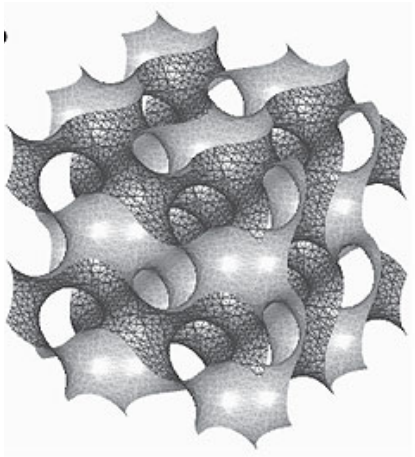

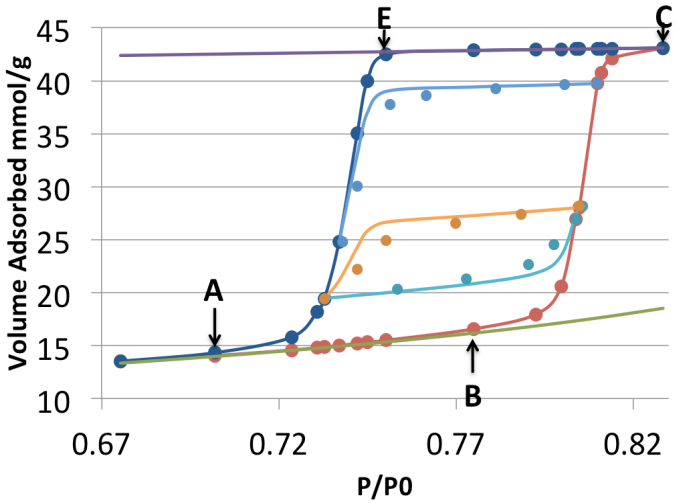

10 nm 3DOm carbon

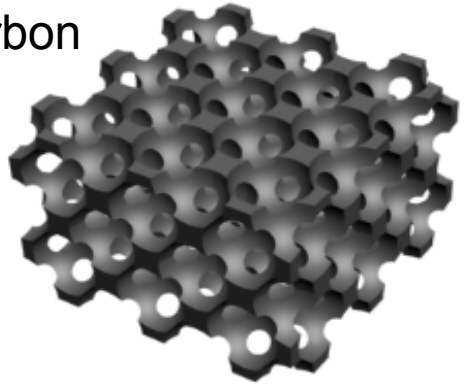

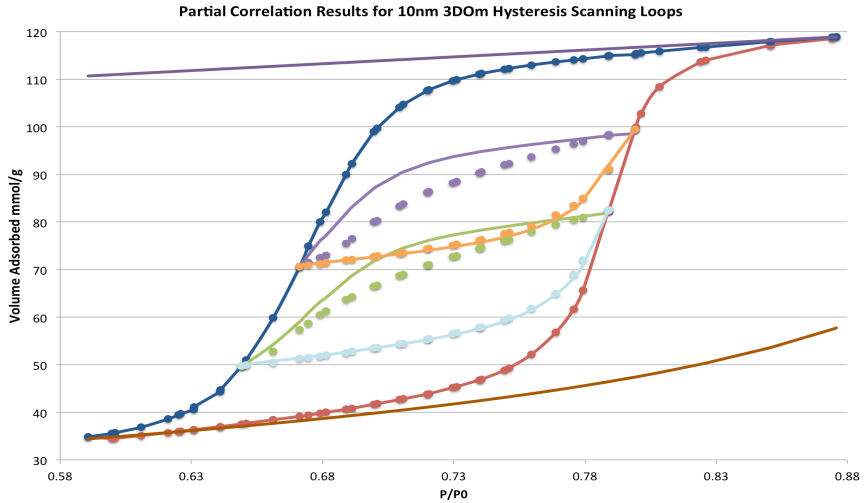

Works for scanning adsorption

Identifies pore blocking/percolation effects during desorption

Partial correlation model provides a test for percolation effects

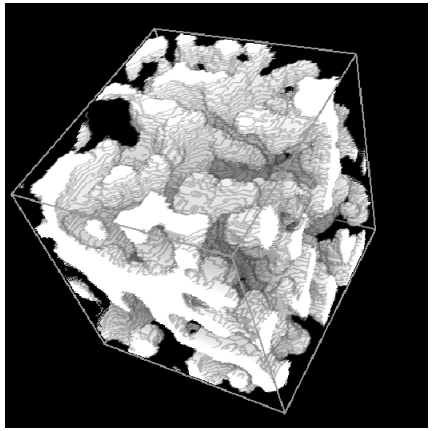

Vycor glass – disordered 3D pore network

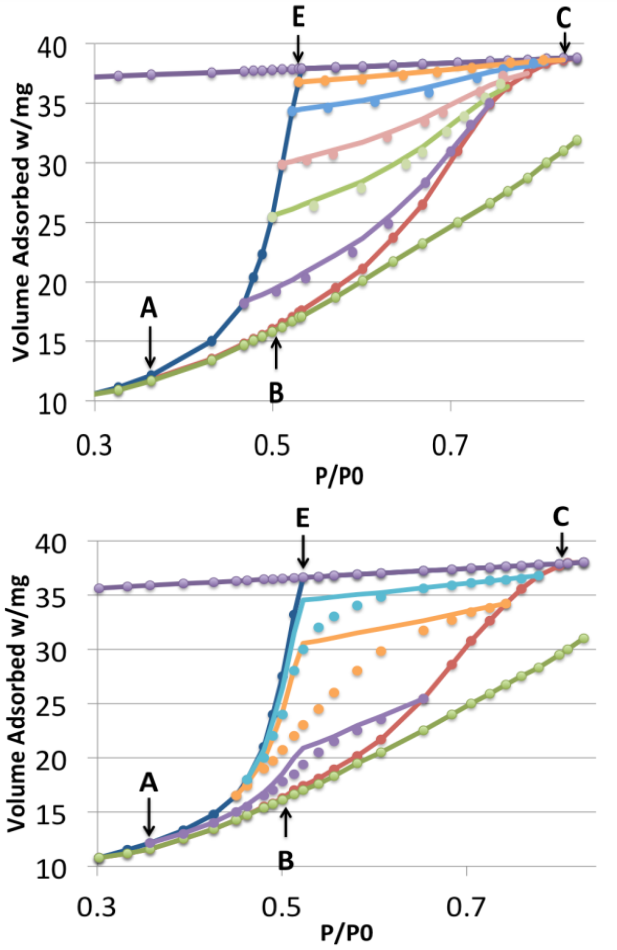

Works for scanning adsorption
Identifies pore blocking/percolation effects during desorption

Percolation Systems

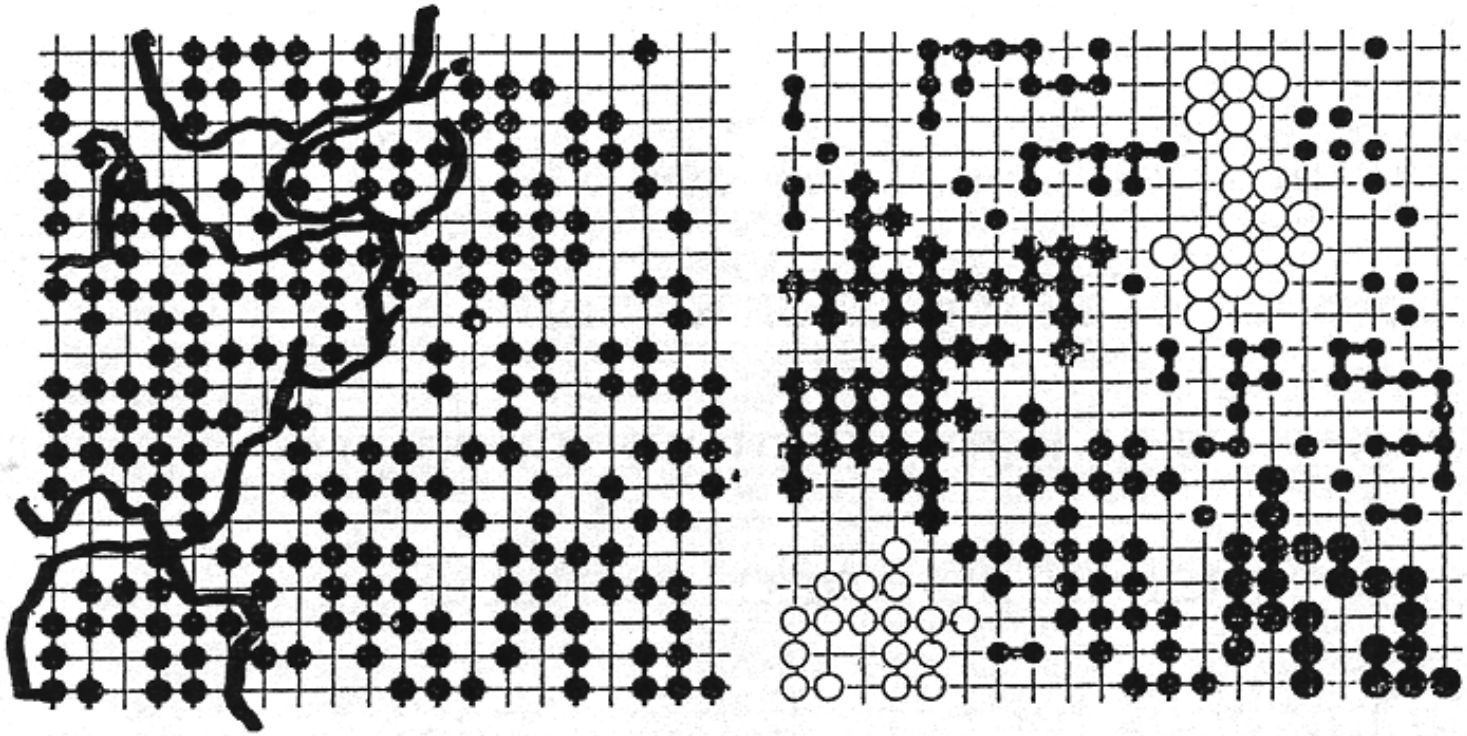

FIGURE 7.1: A quadratic lattice with one half of the nodes occupied by 'pores' is shown to the left. Connected regions, or 'clusters' are shown to the right. The largest clusters are distinguished by using different symbols for the pores. The lattice consists of $L \times L$ nodes with $L = 20$.

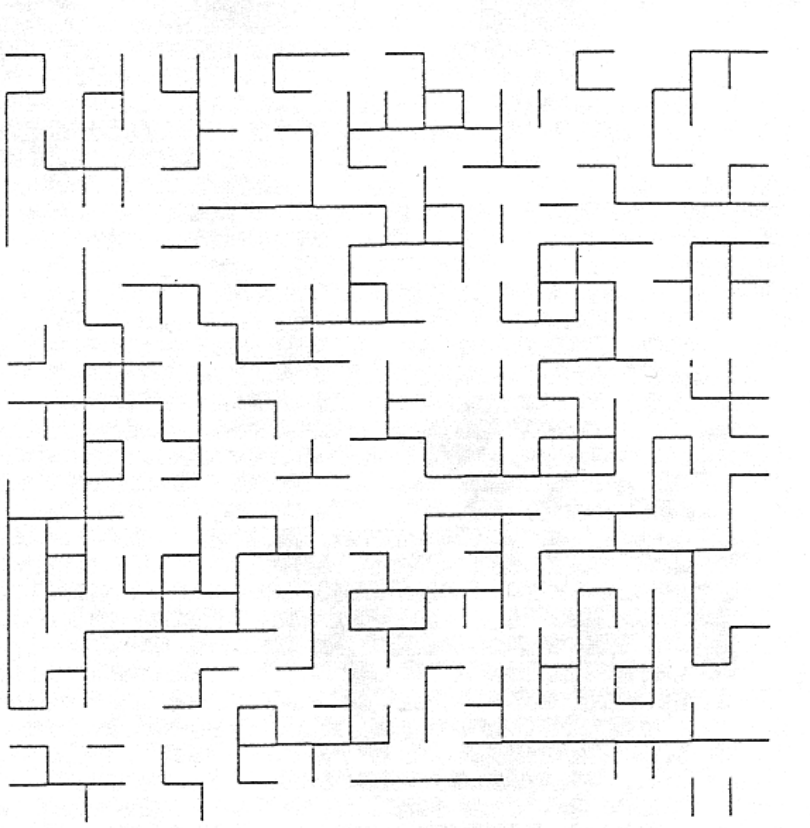

Bond-percolation clusters on a 20 x 20 square lattice

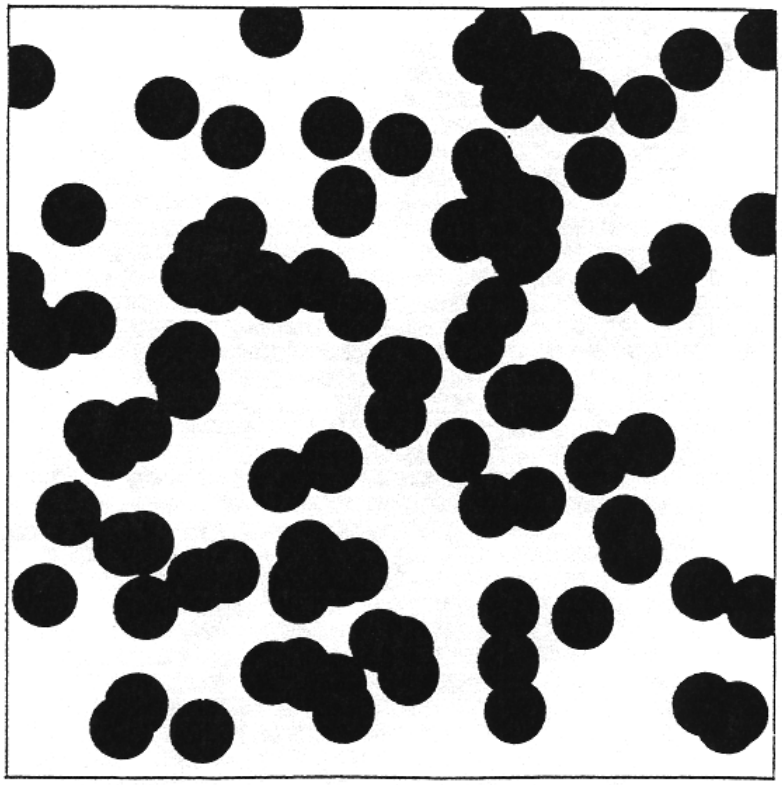

Continuum percolation:Swiss cheese model

3-Dimensional Percolation System

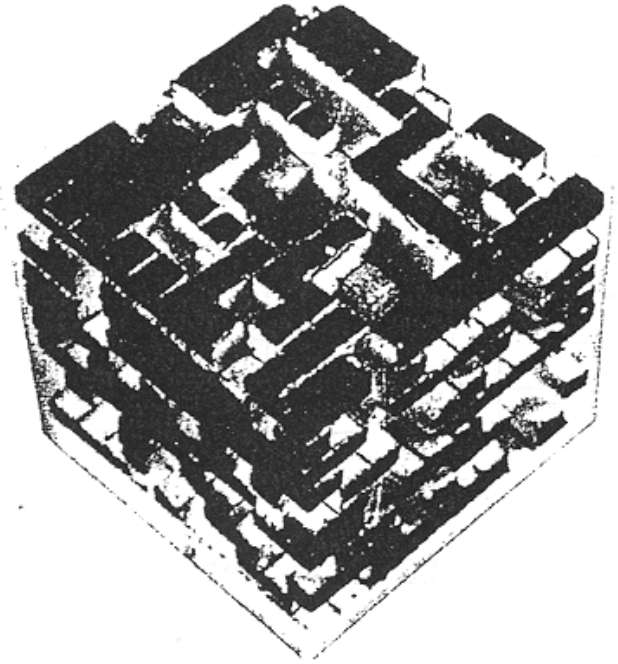

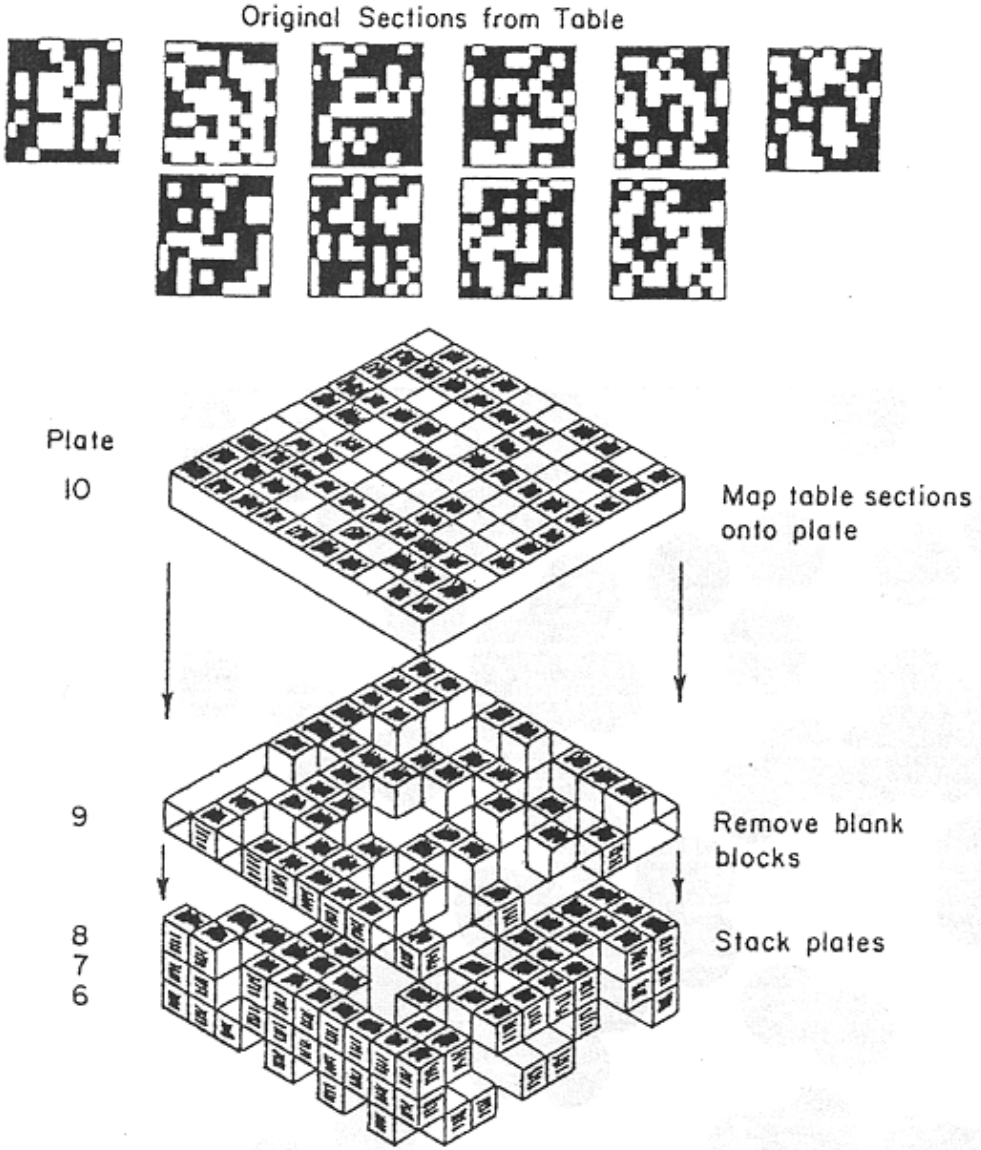

Percolation System on Square Lattice

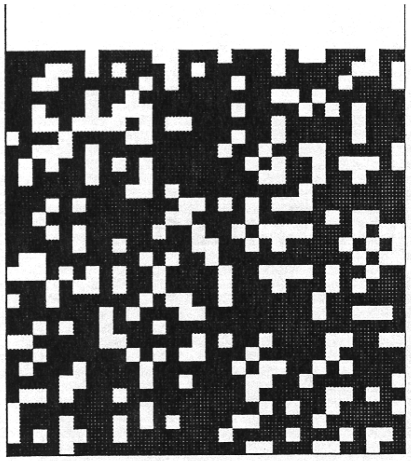

$p = 0.25$
$q = 0.75$

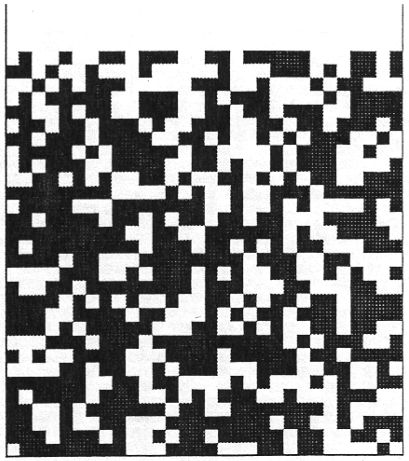

$p = 1 - p_c = 0.41$
$q = p_c = 0.59$

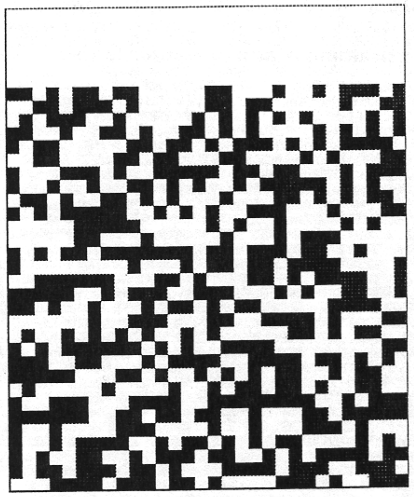

$p = 0.5$
$q = 0.5$

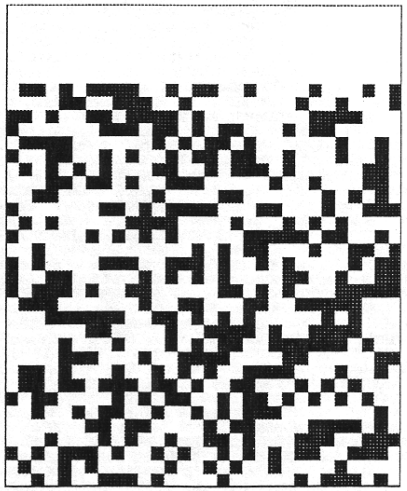

$p = p_c = 0.59$
$q = 1 - p_c = 0.41$

Percolation Probability and Percolation Threshold

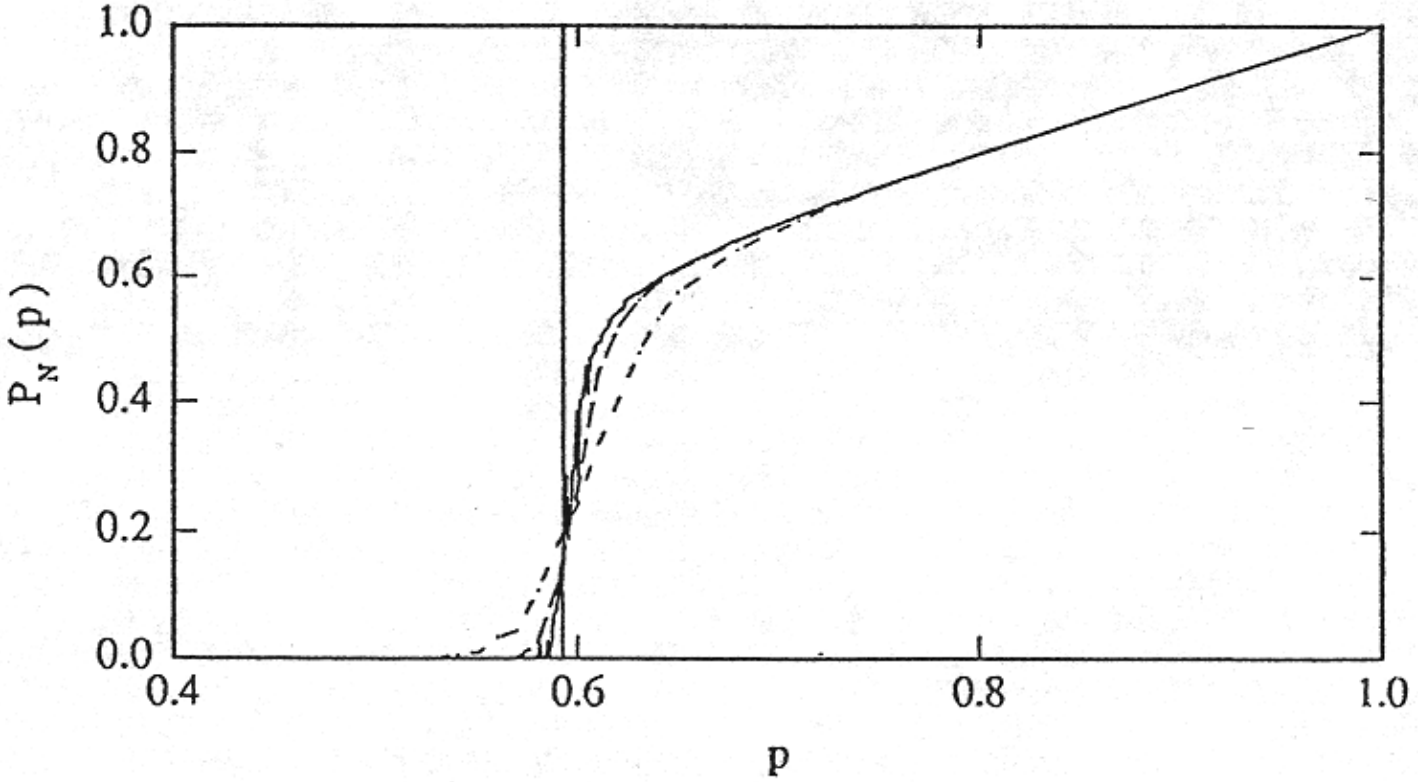

FIGURE 7.3: The probability, $P_N(p)$, of a site belonging to the largest cluster as a function of the probability p that a site is an open pore on an $L \times L$ square lattice. The full curve is obtained for $L = 450$, and the broken lines with $L = 200$ and 50. The vertical line is at $p = p_c = 0.59275$.

Desorption from saturated pore network

Classical bond percolation problem – probability of desorption, or fraction of unfilled pores, $Q(x)$ depends on fraction of metastable necks, $q(x)$.

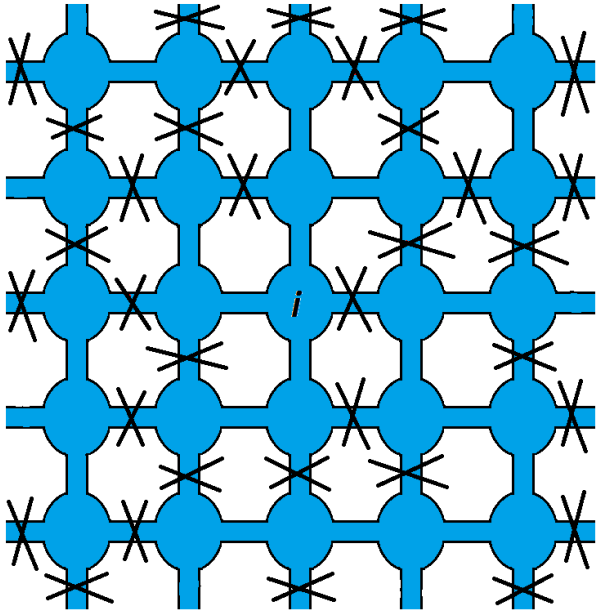

Below percolation threshold

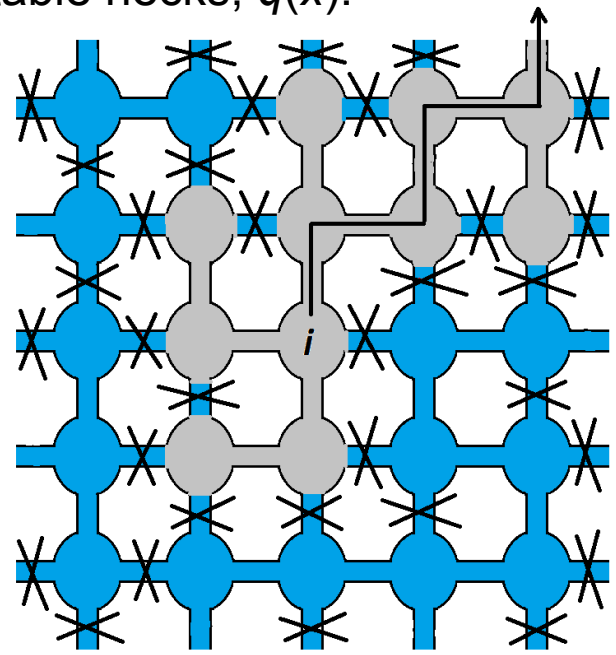

Above percolation threshold

In the process of desorption, condensed fluid can evaporate only from a pore that is connected to the external surface by a continuous path of necks, which contain metastable fluid at given vapor pressure.

Desorption Schematic:
Blue – Condensed fluid.
X – necks with stable fluid at given pressure. Fluid from the pore ***i*** can evaporate along the paths of metastable necks.

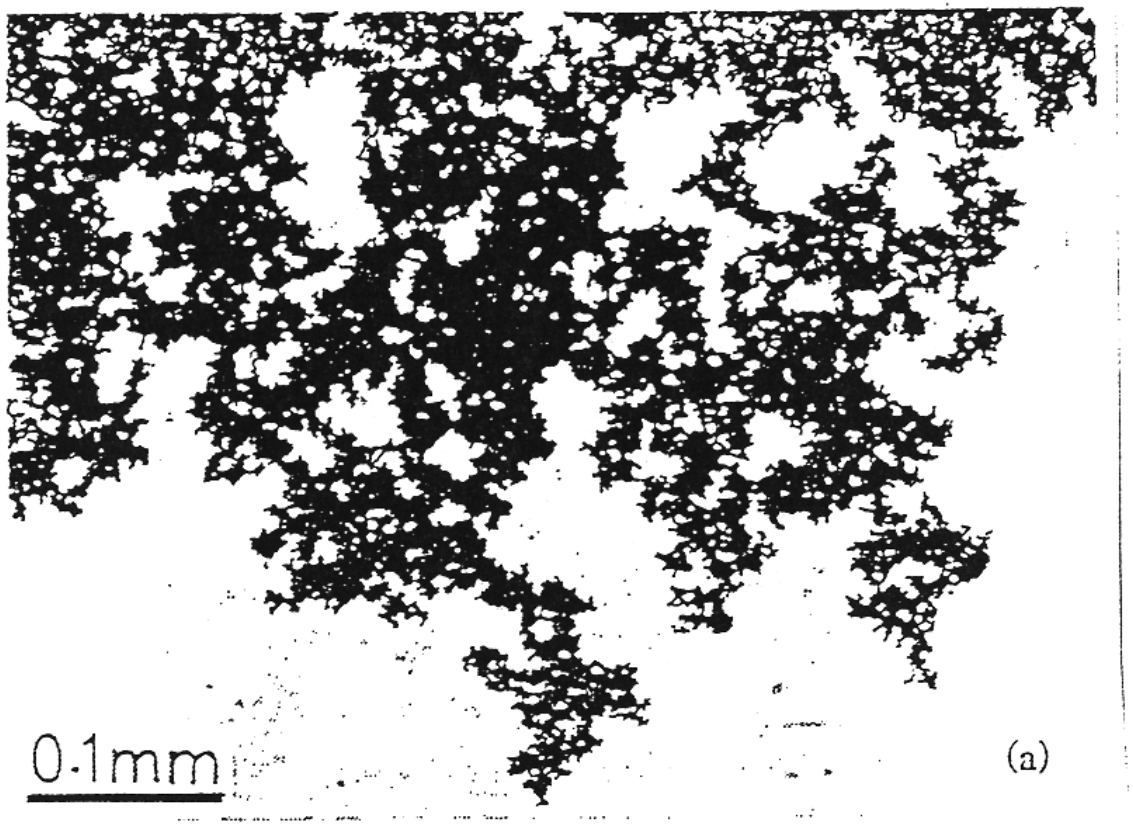

EVAPORATION FROM THE LAYER OF SILICA PARTICLES

Empty pores are dark in the transmitted light image. Filled pores and solid particles are transparent.

T.M.Shaw. Phys.Rev.Lett., 1987, 59, 1671

Desorption from partially saturated pore network

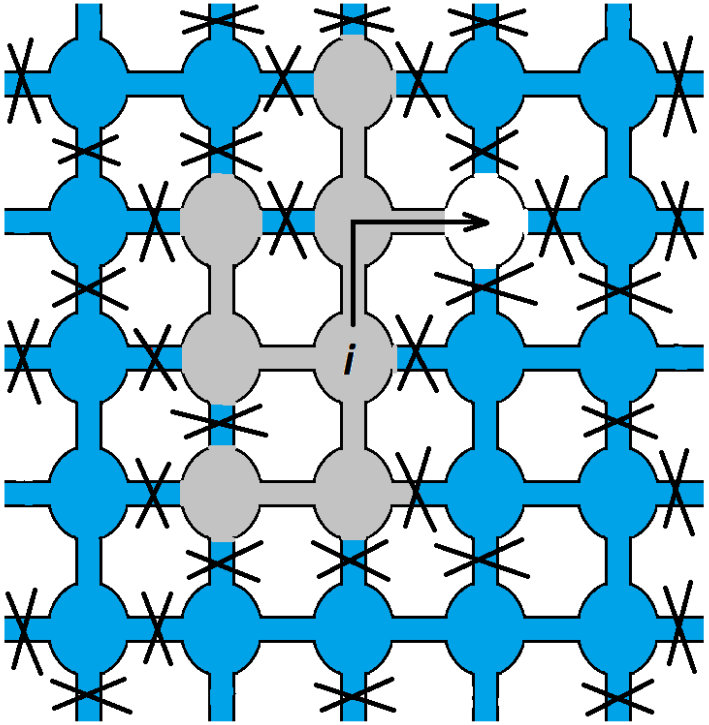

Mixed bond-site percolation problem – probability of desorption, or fraction of unfilled pores, $Q_{-}(x,x_a)$ depends on both, fraction of initially unfilled pores, $Q_{+}(x_a)$, and fraction of metastable necks, $q(x)$. This problem can be solved either by using an analytical approximation (Bethe model), or by direct Monte Carlo simulation.

Bond-site Percolation Model

$$Q_{-}(\chi, \chi_a) = Q_{+}(\chi_a) + \left(1 - Q_{+}(\chi_a)\right) \cdot \alpha(q(\chi), Q_{+}(\chi_a))$$

The fraction of unfilled pores during desorption, $Q_{-}(\chi, \chi_a)$, is determined by the probability factor, $\alpha(q(\chi), Q_{+}(\chi_a))$, which depends on the fraction of unfilled pores in the beginning of scanning, $Q_{+}(\chi_a)$, and the fraction of metastable necks, $q(\chi)$, at given pressure χ.

Bethe approximation: Z – coordination number

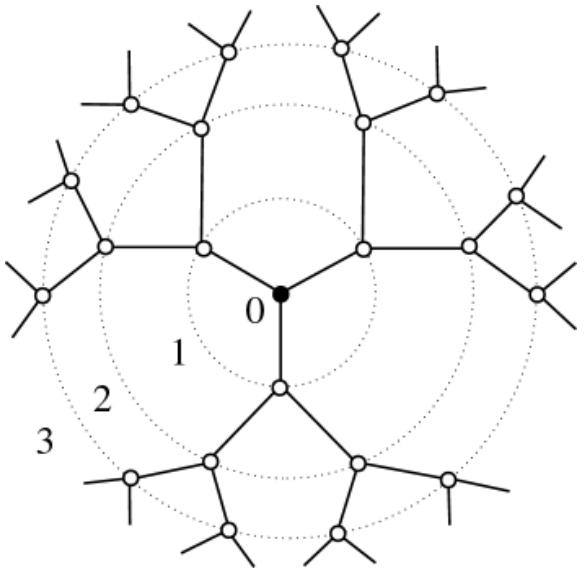

$$\alpha(q, Q_{+}) = 1 - y^{z}$$

y is the probability for given site to be connected with either initially unfilled pore, or with external surface by a continuous path of metastable necks defined by algebraic equation

$$y = (1 - q) + q(1 - Q_{+}) \cdot y^{z-1}$$

Main desorption branch corresponds to $Q_{+} = 0$.

ANV, 1984

Bond-site Percolation Model

$$Q_+(\chi, \chi_d) = Q_+(\chi) \cdot Q_-(\chi_d) \qquad Q_-(\chi, \chi_a) = Q_+(\chi_a) + \left(1 - Q_+(\chi_a)\right) \cdot \alpha(q(\chi), Q_+(\chi_a))$$

$$V(\chi) = Q(\chi) \cdot V_s(\chi) + (1 - Q(\chi)) \cdot V_c(\chi)$$

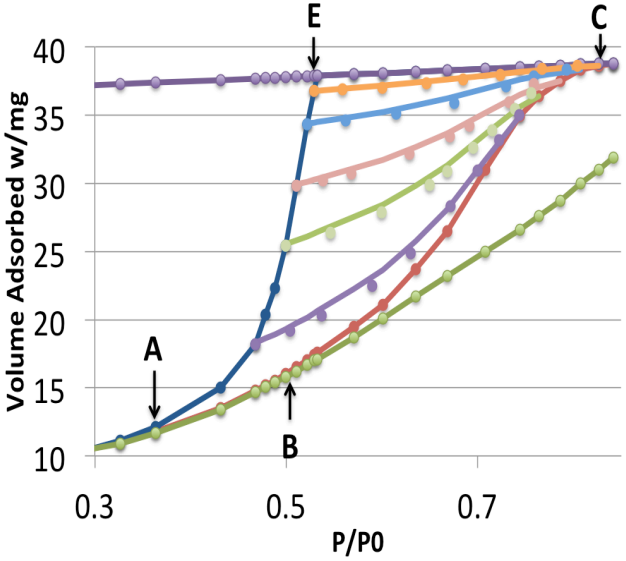

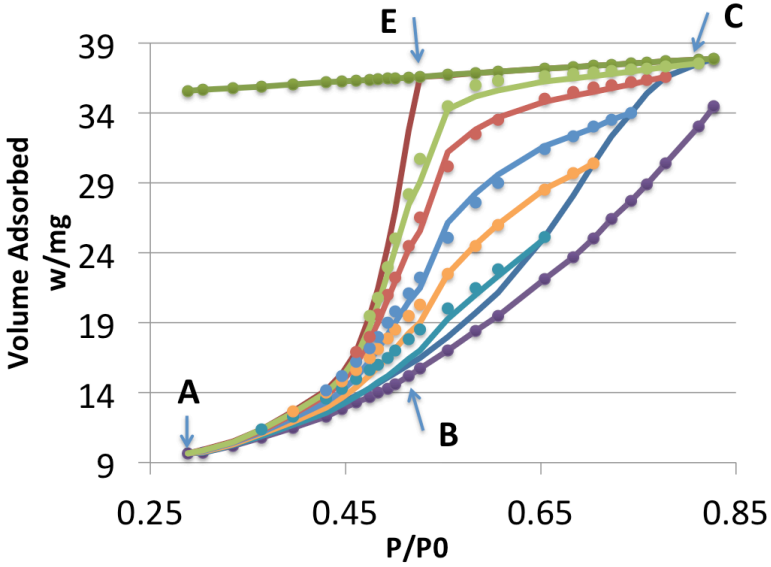

Works for scanning adsorption and desorption for random pore networks like Vycor!

Bond-site Percolation Model – 3D Simulation

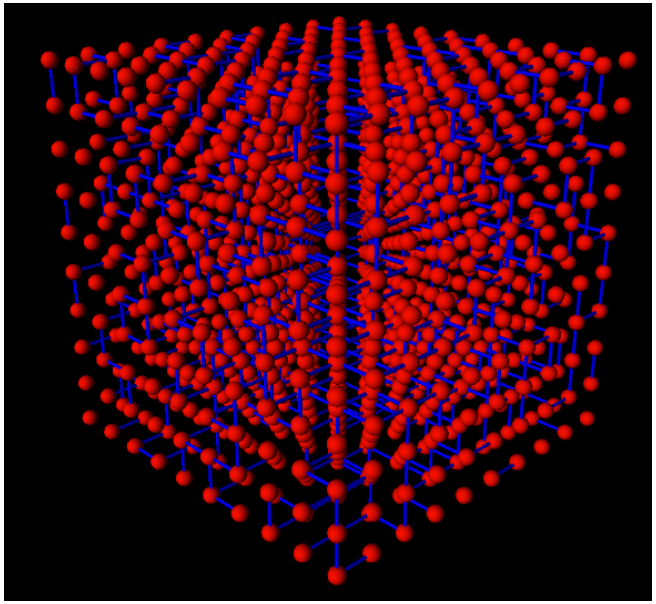

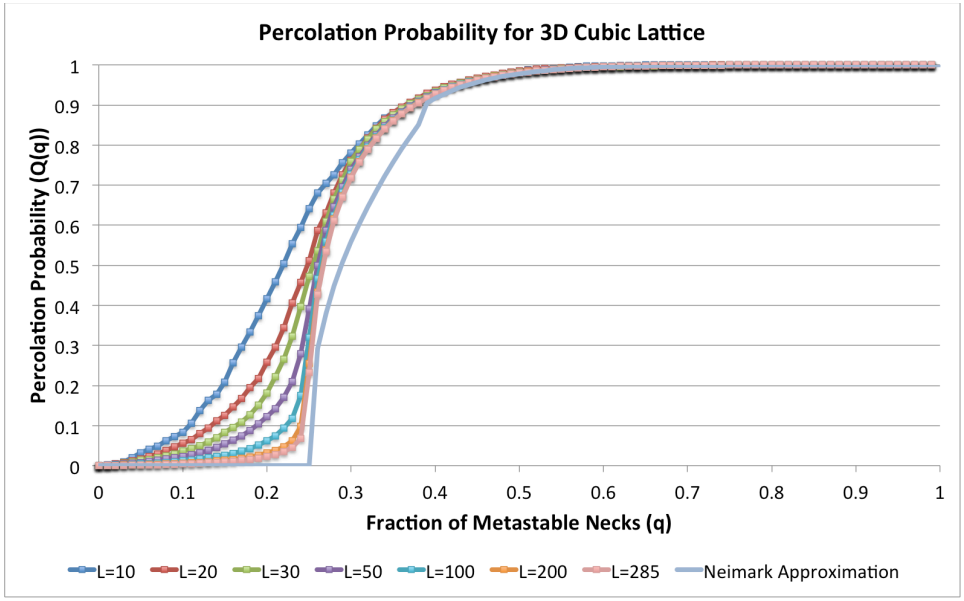

Cubic lattice Z=6, q_c=0.25
Sites – red spheres
Metastable necks – blue lines
Stable necks – blank.
Simulation by modified algorithm of Newman&Ziff (2001).
Shown distribution at q = 0.3.

Dependence of the percolation probability on the network size. 200x200x200 is chosen For further simulations

Rich Cimino, 2012

Bond-site Percolation Model – 3D Simulation

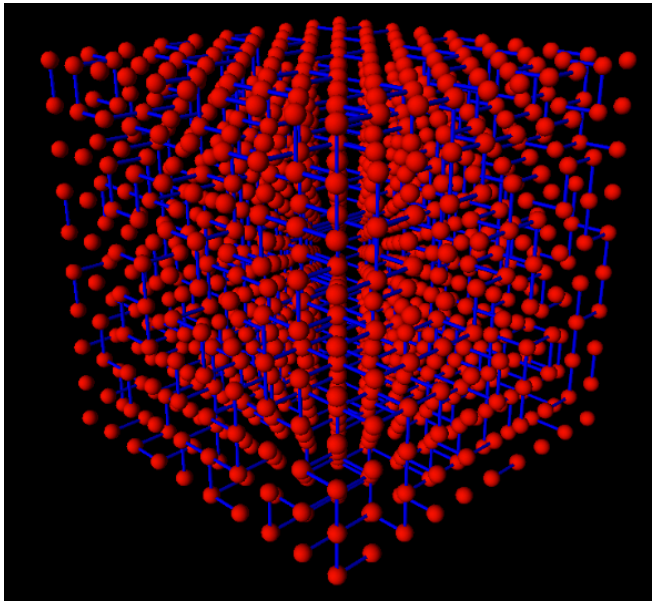

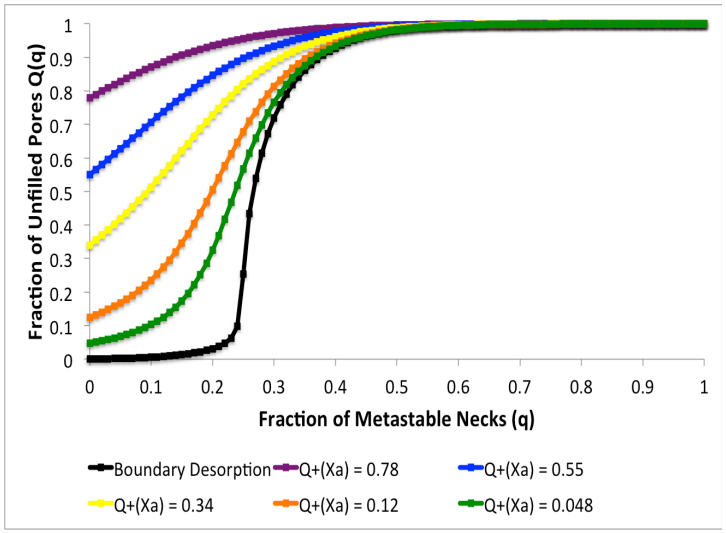

Fraction of unfilled pores $Q_{-}(q, Q_{+})$
Cubic network 200x200x200

Cubic lattice Z=6, q_c=0.25
Sites – red spheres
Metastable necks – blue lines
Stable necks – blank.
Simulation by modified algorithm of Newman&Ziff (2001).
Shown distribution at q = 0.3.

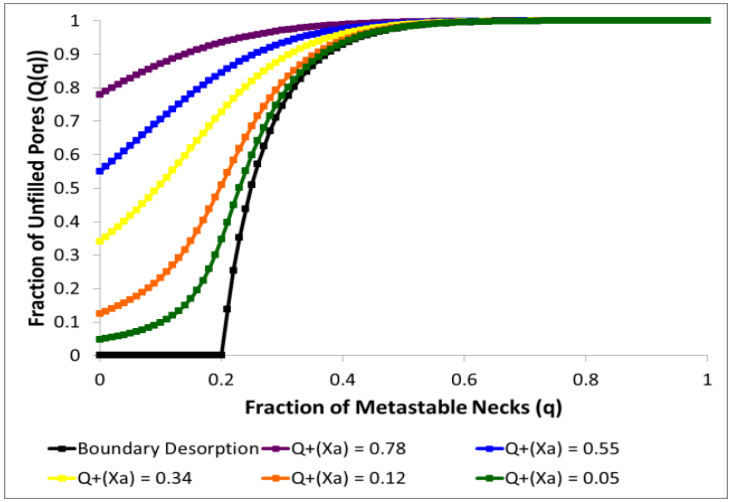

Rich Cimino, 2012

Compare with Bethe approximation, Z=6

Calculating network connectivity and pore size distribution

$$Q_{-}(\chi, \chi_a) = Q_{+}(\chi_a) + \left(1 - Q_{+}(\chi_a)\right) \cdot \alpha(q(\chi), Q_{+}(\chi_a))$$

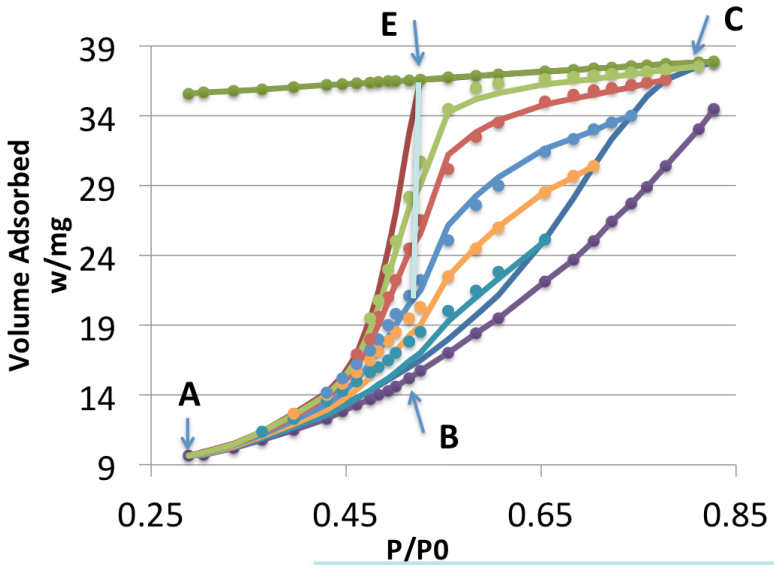

Point E determines the neck size that corresponds to percolation threshold, $q(r_E) = q_c$.

Percolation threshold is determined by network connectivity,
q_c=1.5/Z – 3D lattice; q_c=1/(Z-1) – Bethe lattice

For Vycor: Z=6.8 +/- 0.3

$$Q_{-}(\chi_E|\chi_a) = Q_{+}(\chi_a) + \left(1 - Q_{+}(\chi_a)\right) * \alpha(q_c, Q_{+}(\chi_a)) = \frac{Vc(\chi_E) - V_{-}(\chi_E|\chi_a)}{V_c(\chi_E) - V_s(\chi_E)}$$

theoretical = experimental

Pore size distribution is determined from main adsorption isotherm $Q_{-}(\chi_d)$
Neck size distribution at r<r_E is determined from main desorption isotherm $Q_{-}(\chi)$
Neck size distribution at r>r_E is determined from scanning desorption isotherm $Q_{-}(\chi, x_a)$

Calculating network connectivity and pore size distribution

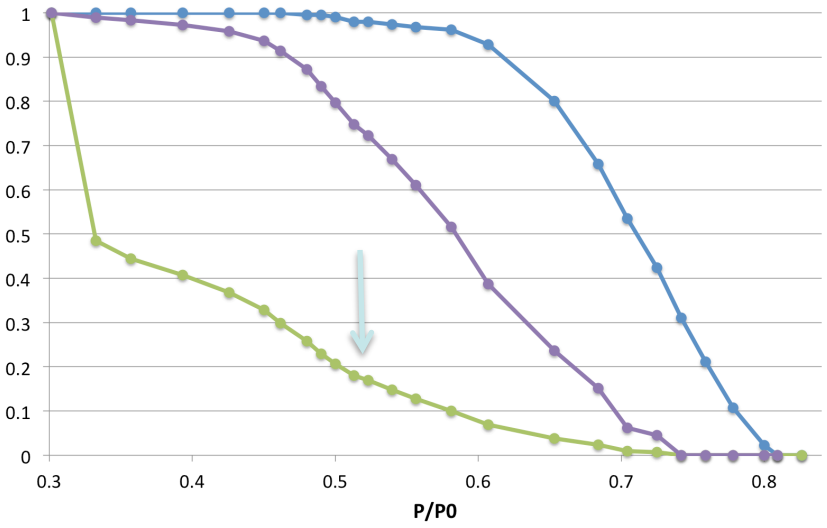

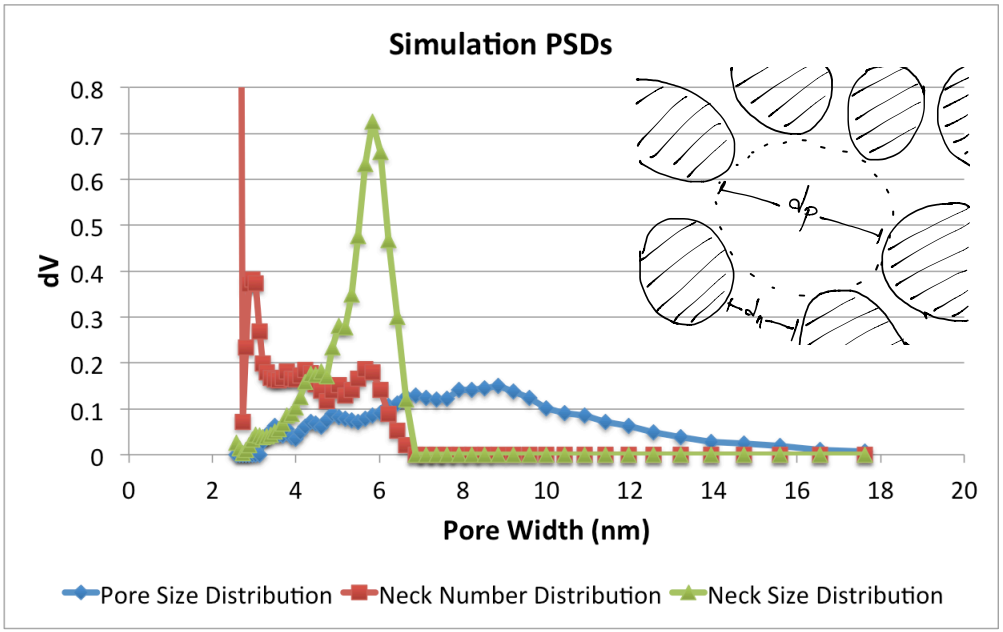

Normalized Pore Size Distributions in Vycor, Z=6.6

Blue – pore distribution by pore size;

Red – number distribution of neck size;

Green – pore distribution by maximum neck size

– suggested method for neck size analysis

Arrow shows the percolation threshold

Calculation from percolation model from Xe scanning adsorption-desorption data [Everett, 1967].

3DOm carbons: network connectivity & pore size distribution

10 nm Carbon, Z_{Bethe}=6.5

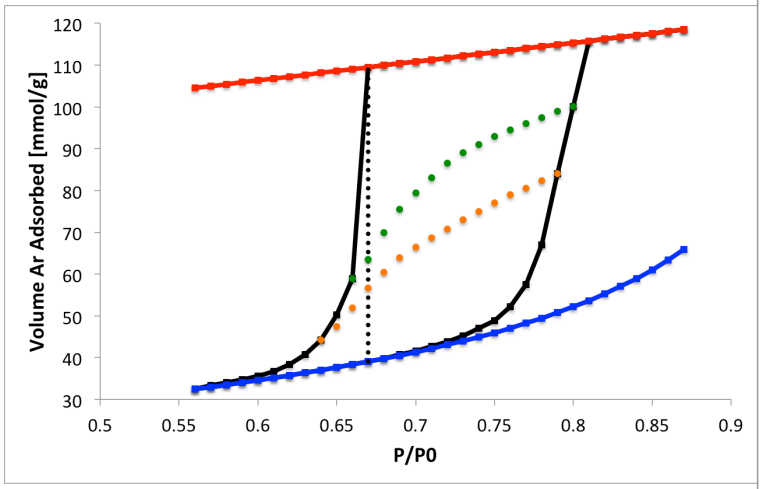

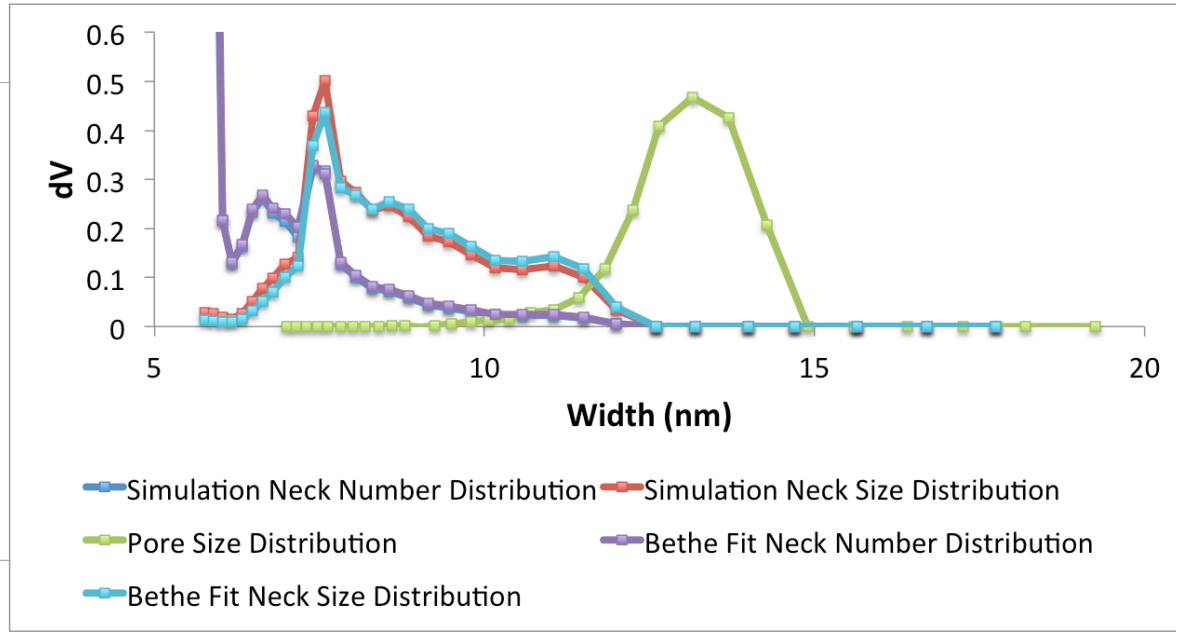

Ar isotherm

QSDFT distributions using cylindrical equilibrium kernel for necks and spherical adsorption kernel for pores.

Wide distribution of neck sizes with small overlap with cage sizes.
Surprisingly, PSDs from the fitted Bethe approximation nicely overlap with calculated from 3D simulation.

3DOm carbons: network connectivity & pore size distribution

20 nm Carbon, Z_{Bethe}=6.7

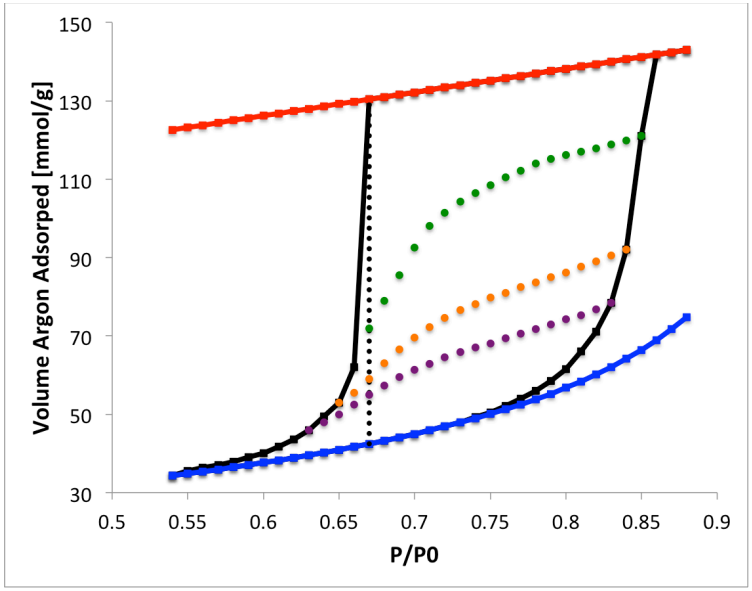

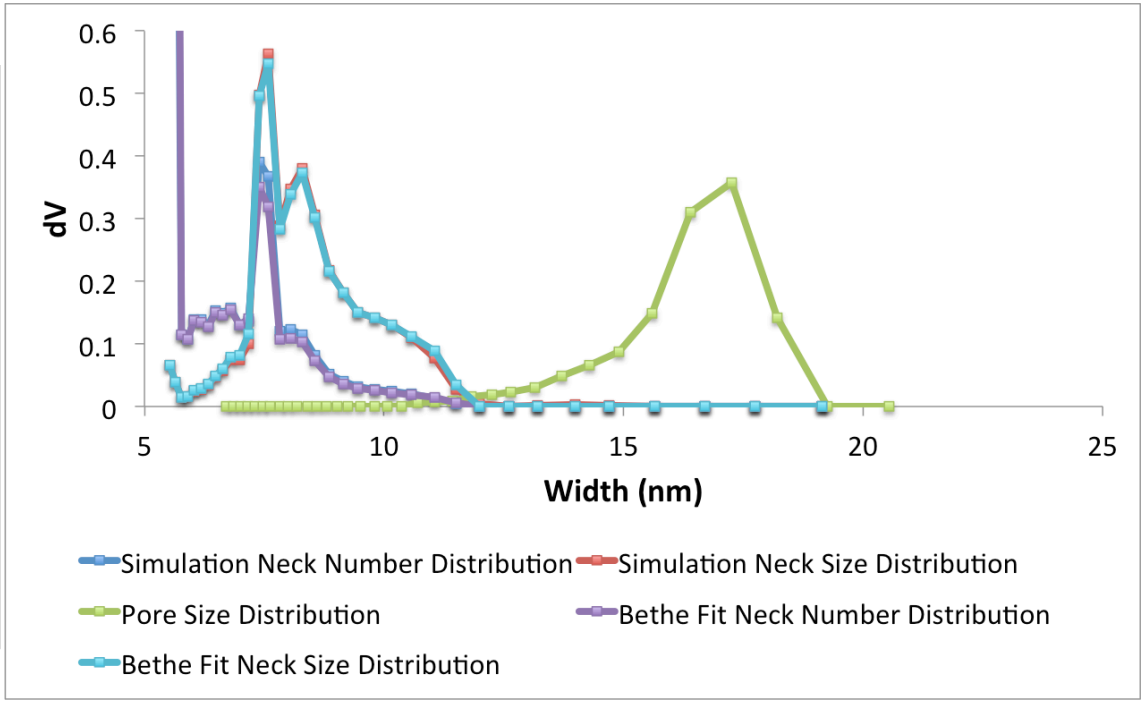

Ar isotherm, green scanning isotherm used for PSD calculations

QSDFT distributions using cylindrical equilibrium kernel for necks and spherical adsorption kernel for cages.

Wide distribution of neck sizes, no overlap with cage sizes.
PSDs from Bethe approximation nicely overlap with calculated from 3D simulation.

3DOm carbons: network connectivity & pore size distribution

30 nm Carbon, Z_{bethe}=5.2

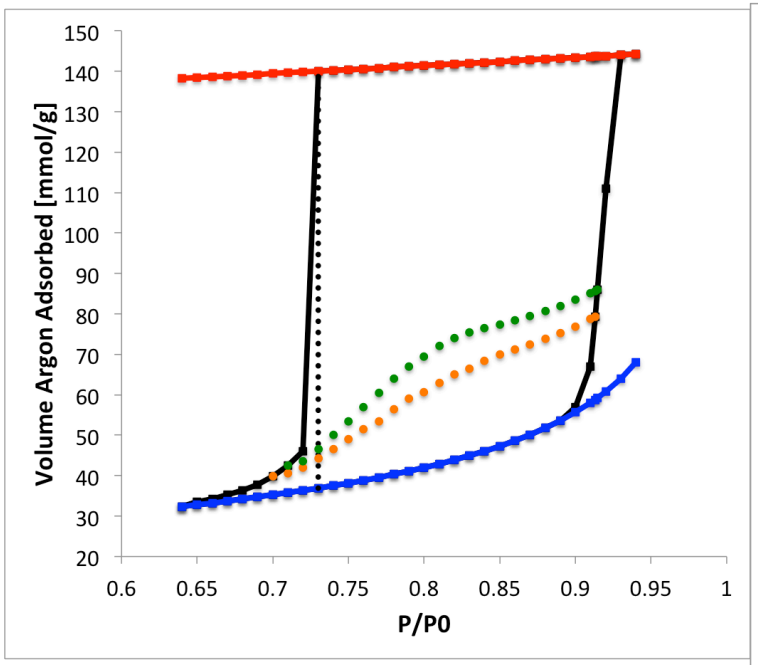

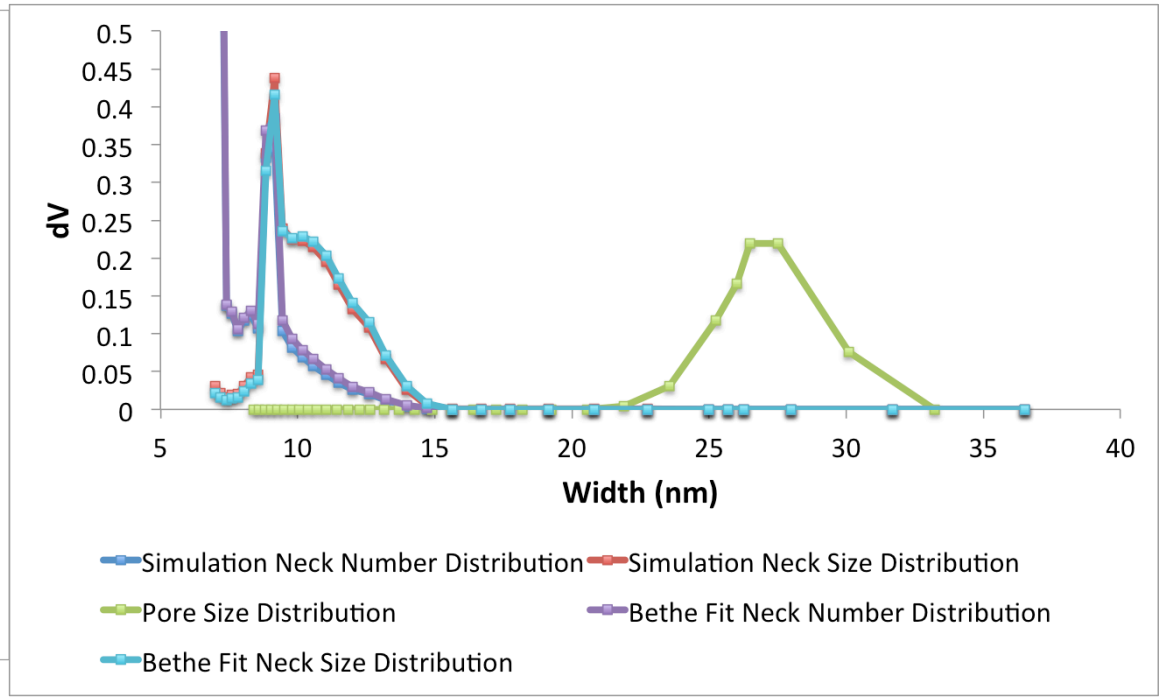

Ar isotherm, green scanning isotherm used for PSD calculations

QSDFT distributions using cylindrical equilibrium kernel for necks and spherical adsorption kernel for cages.

Wide distribution of neck sizes, no overlap with cage sizes.
PSDs from Bethe approximation nicely overlap with calculated from 3D simulation.

3DOm carbons: network connectivity & pore size distribution

40 nm Carbon, Z_{bethe}=5.1

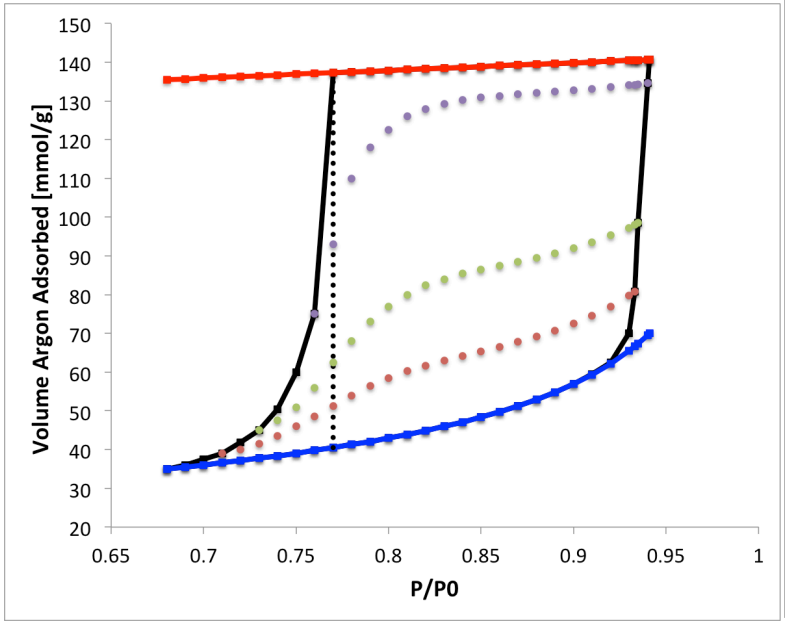

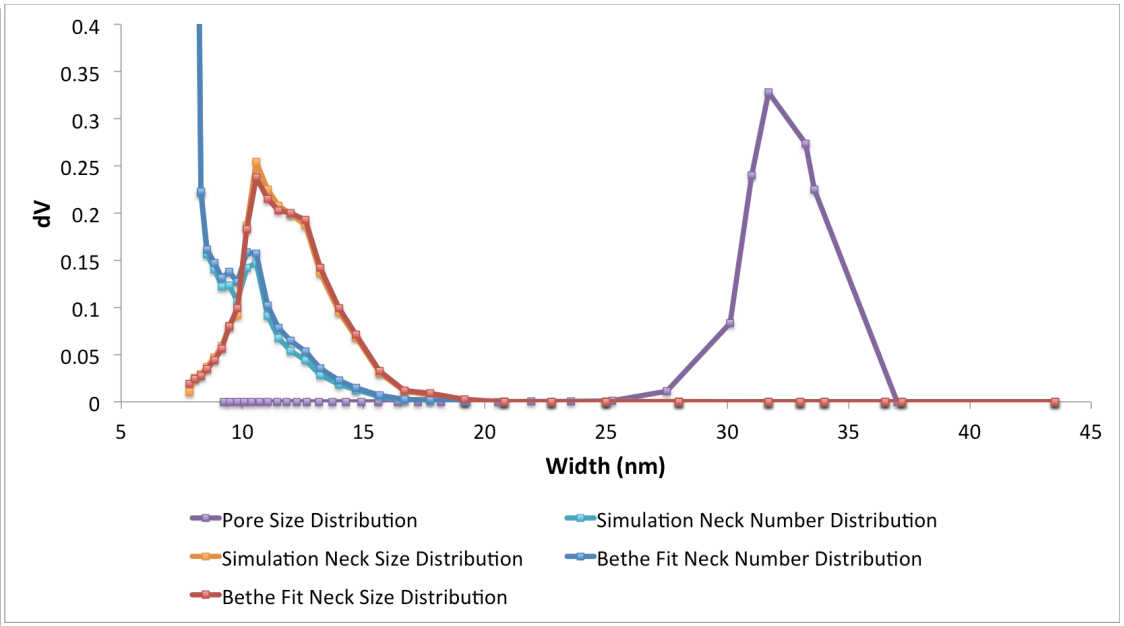

Ar isotherm with the secondary structure subtracted, upper scanning isotherm used for calculations

QSDFT distributions using cylindrical equilibrium kernel for necks and spherical adsorption kernel for cages.

There is a well defined separation between the pores and necks

Evaporation (desorption) from a network of pores is geometrically similar to drainage and intrusion of a non-wetting fluid (mercury) - percolation transition

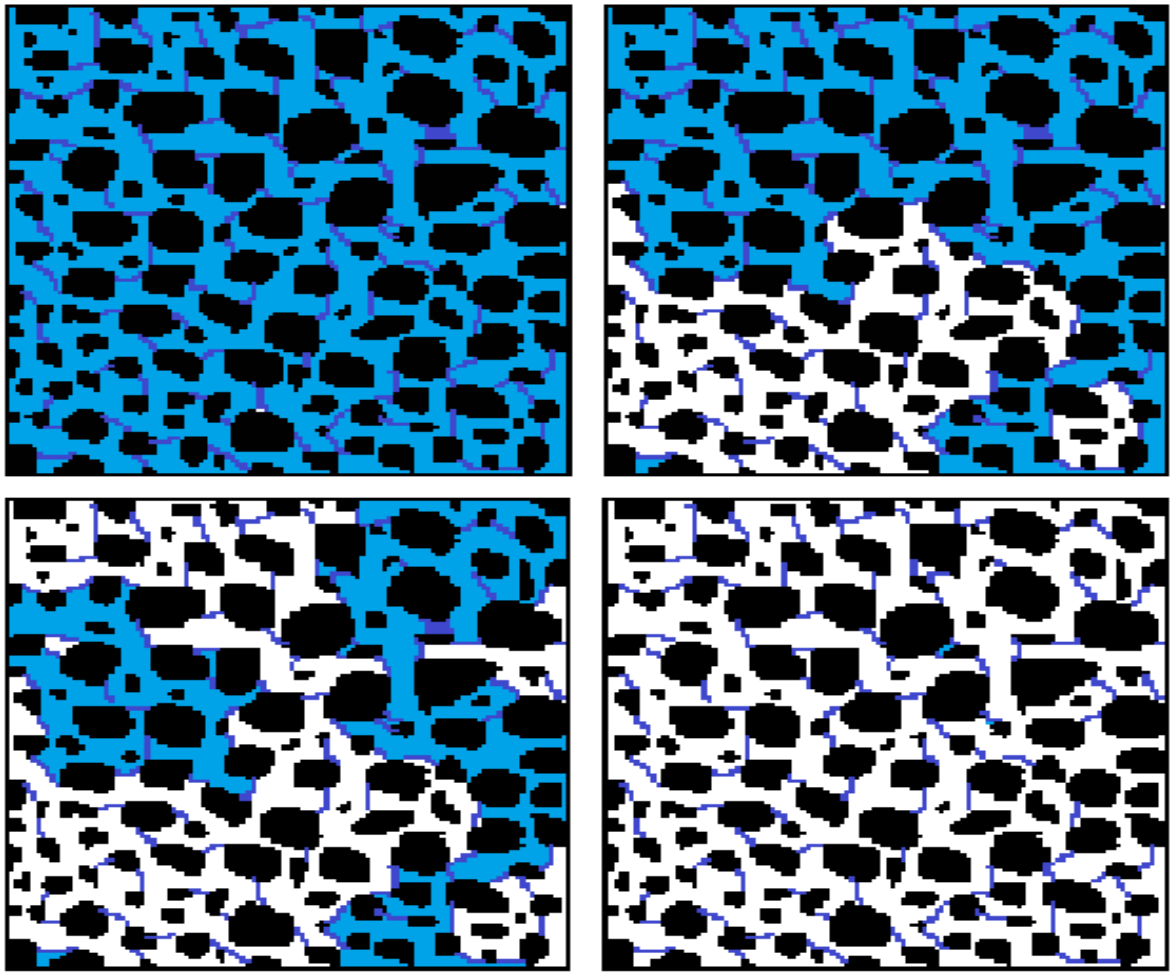

AVN, COPS-II, 1990

Network models are applicable to various hysteresis processes

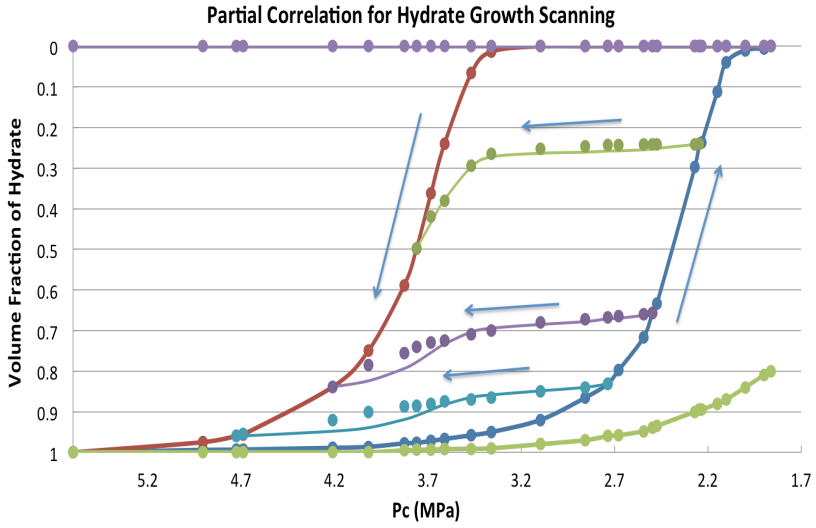

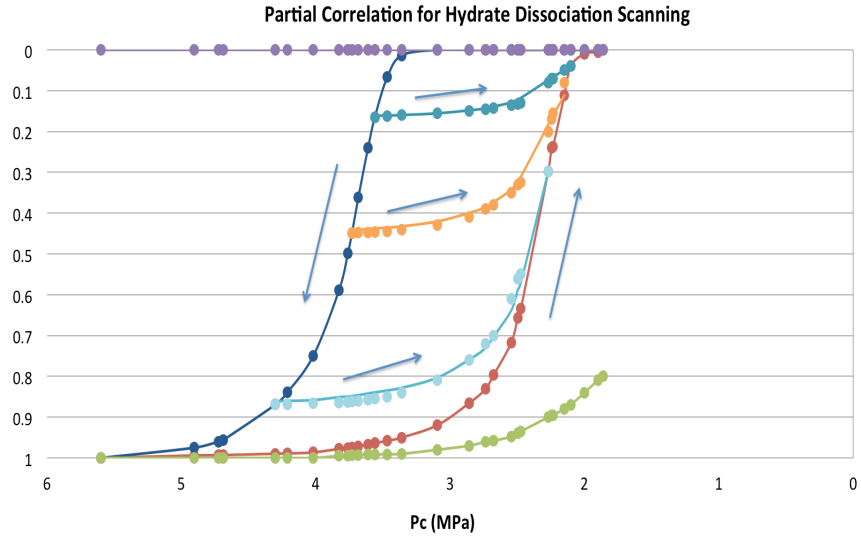

Gas Hydrate Crystal Growth and Dissociation Hysteresis

The hysteresis phenomena which occur in gas hydrate crystal growth in porous silica sediments can be treated with the partial correlation model with relative accuracy. The arrows show the directionality of the hysteresis loops during experiment. Left and downwards are hydrate growth, while right and upwards represents hydrate dissociation.

Andersen et al, 2011

Conclusions

- Scanning isotherms contain valuable information about the pore network connectivity and pore size distribution

- Partial Correlation model provides a test for pore blocking effects

- Percolation model is suggested to determine:
  - connectivity as an effective coordination number of pore network
  - distribution for pore and neck sizes

- 3D network simulation is in agreement with Bethe approximation in terms od calculated PSD

- New information about the pore structure of reference (SBA-15, KIT-6, and Vycor) and novel (3DOm silica) materials.

Credits:

Richard Cimino, Rutgers University
Katie Cychosz and Matthias Thommes, Quantachrome

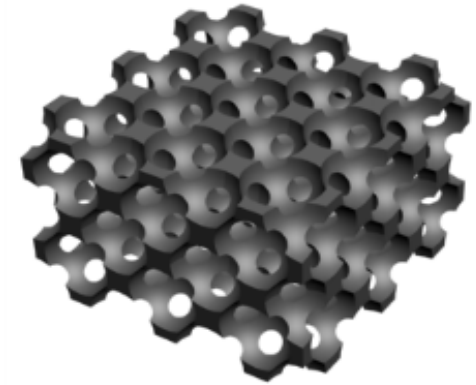

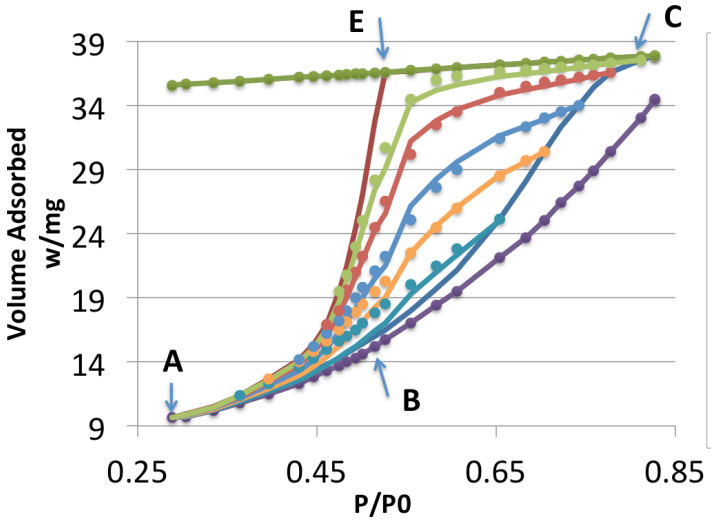

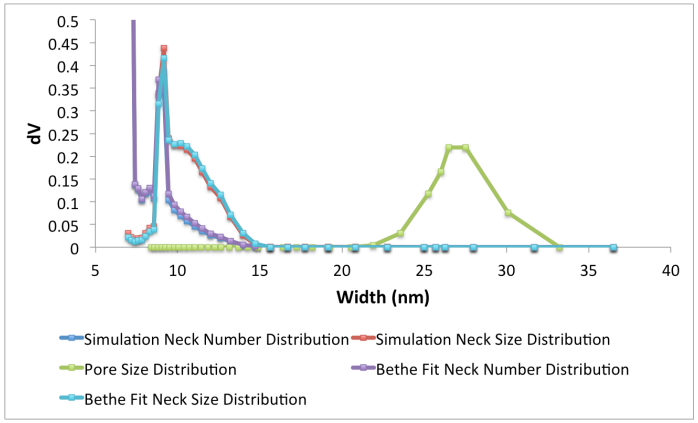

**Funding: Blaise Pascal International Chair,
NSF ERC on Structural Organic Particulate Systems**